

 Open access • Journal Article • DOI:10.1002/2017JD027418

Trends and Variability of Surface Solar Radiation in Europe Based On Surface- and Satellite-Based Data Records — [Source link](#)

Uwe Pfeifroth, Arturo Sanchez-Lorenzo, Arturo Sanchez-Lorenzo, V. Manara ...+2 more authors





Institutions: Deutscher Wetterdienst, University of Extremadura, Spanish National Research Council

Published on: 16 Feb 2018 - Journal of Geophysical Research (John Wiley & Sons, Ltd)

Topics: Satellite

Related papers:

- [Global dimming and brightening: A review](#)
- [Decadal changes in radiative fluxes at land and ocean surfaces and their relevance for global warming](#)
- [Reassessment and update of long-term trends in downward surface shortwave radiation over Europe \(1939–2012\)](#)
- [Trends in downward surface solar radiation from satellites and ground observations over Europe during 1983–2010](#)
- [Digging the METEOSAT Treasure—3 Decades of Solar Surface Radiation](#)

Share this paper:    

View more about this paper here: <https://typeset.io/papers/trends-and-variability-of-surface-solar-radiation-in-europe-18j9yt4iso>

1 Trends and Variability of Surface Solar Radiation in
2 Europe based on Surface- and Satellite-based Data
3 Records

Uwe Pfeifroth¹, Arturo Sanchez-Lorenzo², Veronica Manara^{3,4}, Jörg
Trentmann¹ and Rainer Hollmann¹

Corresponding author: Uwe Pfeifroth, Satellite-based Climate Monitoring, Deutscher Wetter-
dienst, Offenbach, Germany. (uwe.pfeifroth@dwd.de)

¹Satellite-based Climate Monitoring,
Deutscher Wetterdienst, Offenbach,
Germany.

²Pyrenean Institute of Ecology (IPE),
Spanish National Research Council (CSIC),
Zaragoza, Spain

³Department of Physics, Università degli
Studi di Milano, Milan, Italy.

⁴Now at: Institute of Atmospheric
Sciences and Climate, ISAC-CNR, Bologna,
Italy.

Abstract.

The incoming solar radiation is the essential climate variable that determines the Earth's energy cycle and climate. As long-term high-quality surface measurements of solar radiation are rare, satellite data are used to derive more information on its spatial pattern and its temporal variability. Recently, the EUMETSAT Satellite Application on Climate Monitoring (CM SAF) has published two new satellite-based climate data records: Surface Solar Radiation Dataset - Heliosat, Edition 2 (SARAH-2) and Clouds and Radiation Dataset based on AVHRR Satellite Measurements, Edition 2 (CLARA-A2). Both data records provide estimates of surface solar radiation. In this study, these new climate data records are compared to surface measurements in Europe during the period 1983-2015. SARAH-2 and CLARA-A2 show a high accuracy compared to ground-based observations (mean absolute deviations of 6.9 and 7.3 W/m^2 respectively) highlighting a good agreement considering the temporal behavior and the spatial distribution. The results show an overall brightening period since the 1980's onwards (comprised between 1.9 and 2.4 $W/m^2/decade$), with substantial decadal and spatial variability. The strongest brightening is found in Eastern Europe in spring. An exception is found for Northern and Southern Europe, where the trends shown by the station data are not completely reproduced by satellite data, especially in summer in Southern Europe. We conclude that the major part of the observed trends in surface solar radiation in Europe is caused by changes in clouds and that remaining differences between the satellite- and the station-based

²⁷ data might be connected to changes in the direct aerosol effect and in snow

²⁸ cover.

1. Introduction

29 Solar radiation is an essential climate variable ECV and the main energy source for the
30 Earth-Atmosphere system [Wild et al., 2015; Ohmura and Gilgen, 1993; Ramanathan et
31 al., 2001]. High-quality and long term measurements of the solar radiation are of major
32 importance for our understanding of the climate system [Hartmann et al., 1986]. Further,
33 surface solar radiation (SSR) is a main constitute for the surface radiation budget [Wild
34 et al., 2017] that e.g. determines the temperatures of the troposphere. Moreover the SSR
35 is of high importance not only for climate studies but also for many other applications
36 e.g. solar energy production [Wild et al., 2015; Huld et al., 2017; Miglietta et al., 2017],
37 agriculture [Stanhill and Cohen, 2001] and vegetations dynamics [e.g. Mercado et al.,
38 2009].

39 Available studies document a widespread reduction ($3 - 9 W/m^2$) of SSR from the
40 1950s to the 1980s called "global dimming" [Stanhill and Cohen, 2001] and a subsequent
41 increase ($1 - 4 W/m^2$) since the 1980s called "brightening" [Wild et al., 2005; Gilgen et
42 al., 2009; Wild, 2009]. These variations are mostly due to changes in the transparency of
43 the atmosphere due to variations in cloudiness and/or changes in anthropogenic aerosol
44 emissions [Liepert et al., 1994; Stanhill and Cohen, 2001; Wild, 2009; Wild et al., 2016].
45 However, the full understanding of the mechanisms and the contributions of both phe-
46 nomena to the observed chnages are still have some uncertain due to for example the
47 lack of long-term SSR data, especially over ocean, remote land areas (e.g., Africa and
48 Siberia) and areas characterized by complex orography (e.g. the Alpine region) [Wild,
49 2009, 2012; Sanchez-Lorenzo et al., 2015]. Here, data from satellite observations (e.g.,

50 those provided by the EUMETSAT Satellite Application Facility on Climate Monitoring
51 - CMSAF) provide valuable additional information [Schulz *et al.*, 2009], as they deliver
52 an unique spatial coverage since the 1980s for both land and oceans [Hinkelmann *et al.*,
53 2009; Zhang *et al.*, 2015; Raschke *et al.*, 2016; Karlsson *et al.*, 2017b].

54 The highest quality of ground-based measurements of SSR are collected in the Baseline
55 Surface Radiation Network (BSRN) Archive [Ohmura *et al.*, 1998]. Unfortunately, glob-
56 ally there are only about 50 BSRN stations available and their temporal coverage starts
57 on in 1992. Therefore, BSRN cannot be used to evaluate variability and trends given
58 by the satellite records on climatological scale. For Europe, several long-term station
59 measurements are available and have been used already for the analysis of trends and
60 changes, the Global Energy Budget Archive - GEBA [Wild *et al.*, 2017; Sanchez-Lorenzo
61 *et al.*, 2017], the World Radiation Data Center - WRDC and measurements provided and
62 managed by individual countries [e.g. Sanchez-Lorenzo *et al.*, 2013; Manara *et al.*, 2016]).

63 Satellite-based data of SSR from the CMSAF has been validated by Urraca *et al.* [2017]
64 in Europe using station measurements from national and international databases. It was
65 found that the CMSAF satellite-based SSR data is of a high quality. Sanchez-Lorenzo *et al.*
66 *et al.* [2017] used European station data and a former version of the CMSAF satellite data
67 of SSR to validate trends in Europe during the time period 1983-2010. They found overall
68 positive Trends of SSR in Europe, and largest trends in spring.

69 In this study, two satellite-based climate data records of SSR provided by the CMSAF
70 are evaluated with surface measurement in Europe for the time period 1983-2015 to assess
71 their accuracy and their ability to capture temporal and spatial variability of SSR in
72 Europe. The data and methods used in this study are presented in Section 2 and 3,

73 respectively. A basic evaluation is shown in Section 4 and the trend and variability analysis
74 are shown in Section 5. The discussion of results and conclusions are presented in Section 6.

2. Data

75 The data used in this study are **two** climate data records generated by the CM SAF,
76 **namely the** Surface Solar Radiation dataset - Heliosat, Edition 2 (SARAH-2) and the CM
77 SAF Clouds, Albedo and Radiation dataset from AVHRR data - Edition 2 (CLARA-A2).
78 For validation purposes ground-based SSR measurements are used.

2.1. Station data

79 Long-term measurements of SSR are freely available from the Global Energy Budget
80 Archive (GEBA) [*Sanchez-Lorenzo et al., 2015; Wild et al., 2017*], maintained by the
81 ETH in Zurich, Switzerland, and from the World Radiation Data Center (WRDC) in
82 St. Petersburg, Russia (<http://wrdc.mgo.rssi.ru/>). Even though all station data have
83 been subject to a quality control and homogenization procedure, the data used in this
84 study has been additionally checked. Additional measurements from Spain [*Sanchez-*
85 *Lorenzo et al., 2013*] and Italy [*Manara et al., 2016*] are used in this study. Overall,
86 53 stations of monthly SSR measurements over Europe, providing data in the 1983-2015
87 period, have been collected. A list of all stations including further site information is shown
88 in Table 1. Figure 1 shows the map of the analyzed area (Europe) including the station
89 locations. The stations are relatively **equally** distributed (**except** the South-Eastern part
90 of Europe) and cover different climate zones. The stations were further divided into 5
91 regions with similar temporal variability (determined by means of a Principal Component

92 Analysis [*Sanchez-Lorenzo et al.*, 2015]), as indicated in Figure 1. This regionalization of
93 stations allows for a condensed and more robust regional trend analysis.

2.2. Clouds, Albedo and Radiation dataset from AVHRR data - Edition 2

94 The CMSAF Clouds, Albedo and Radiation dataset from AVHRR data - Edition 2
95 (CLARA-A2, [*Karlsson et al.*, 2017a]), covers the time period 1982-2015 and provides
96 radiation and cloud parameters as daily and monthly means. The data record is based
97 on the polar orbiting satellite measurements from the Advanced Very High Resolution
98 Radiometer (AVHRR) and is available globally with a spatial resolution of $0.25^\circ \times 0.25^\circ$.
99 More information about the CLARA-A2 satellite retrieval and the available data records
100 is provided by *Karlsson et al.* [2017b].

101 Beside various cloud information and the surface albedo, the CLARA-A2 climate data
102 record contains up- and downwelling surface longwave radiation as well as SSR. The
103 accuracy of monthly SSR from CLARA-A2 has been assessed by *Karlsson et al.* [2017b].
104 It is found that the monthly mean CLARA-A2 SSR data has a small negative bias of
105 $-1.6 W/m^2$ and a mean absolute bias of $8.8 W/m^2$ with reference to globally distributed
106 station data from BSRN.

107 A known deficiency influencing the quality of SSR in the CLARA-A2 climate data
108 record is the availability of only a single AVHRR instrument at any given time during
109 the 1st decade of the data record (1982-1991). Therefore the spatiotemporal sampling
110 of CLARA-A2 is limited during the early period, which leads to an increased number of
111 missing data to estimate monthly means in the region of interest, reaching up to 50%
112 missing data in Southern Europe. From 1992 onwards the spatiotemporal coverage is
113 more complete. After 1992 the local overpass times of the used polar orbiting satellites

114 are in the morning and afternoon – at about 7.00 and 15.00 local time, respectively. Since
115 2002 a third satellite observes Europe at about 10.00 local time. Detailed information on
116 the satellite orbits can be found in Figure 1 from *Karlsson et al.* [2017b].

2.3. Surface Solar Radiation dataset - Heliosat, Edition 2

117 The Surface Solar Radiation Dataset - Heliosat, Edition 2 (*SARAH-2*, *Pfeifroth et*
118 *al.* [2017]) is the latest CMSAF climate data record of surface radiation based on the
119 geostationary METEOSAT satellite series covering Africa, Europe and the Atlantic Ocean.
120 It is the follow-up of the widely used SARAH climate data record [e.g. *Müller et al.*,
121 2015; *Riihelä et al.*, 2015; *Zäk et al.*, 2015]. SARAH-2 covers the time period 1983-2015
122 and offers global and direct radiation parameters as well as the effective cloud albedo.
123 SARAH-2 is provided as daily and monthly means, and as half-hourly instantaneous data.
124 Furthermore, sunshine duration and spectrally resolved radiation are available [*Kothe*
125 *et al.*, 2017]. SARAH-2 covers the region of -65° to $+65^{\circ}$ in longitude and latitude
126 and offers a high spatial resolution of $0.05^{\circ} \times 0.05^{\circ}$. A thorough overview of the basic
127 retrieval principle of the SARAH climate data record series can be found in *Müller et al.*
128 [2015]. SARAH-2 has been improved over the previous data record SARAH-1 especially
129 by improving the stability in the early years and during the transition from the MVIRI to
130 the SEVIRI instrument in 2006. Further a correction to better account for slant viewing
131 geometries has been applied and topographically-corrected integrated water vapor data
132 has been used.

133 The accuracy of the new SARAH-2 climate data record with reference to BSRN is
134 documented in the CMSAF's Validation Report [*Pfeifroth et al.*, 2017] available at [http:](http://)

135 //www.cmsaf.eu/. A positive bias of $+2 W/m^2$ and an absolute bias of $5.1 W/m^2$ for the
136 monthly mean SARA-2 SSR data has been found.

3. Methods

137 All data records are used as monthly means. For comparisons of the gridded satellite
138 data with the station data, the satellite data is extracted at the station locations, by
139 selecting the satellite pixel in which the station is located. The conducted trend calcula-
140 tions for the data records are based on linear regression analysis and based on monthly
141 anomalies with reference to their long-term monthly means. Trends are analysed at the
142 **spatial and** at the seasonal scale, which provides new insights on the temporal and, in case
143 of the satellite data records, also on the spatial variability. **The seasons are defined as**
144 **follow: winter (DJF: December, January, February), spring (MAM: March, April, May),**
145 **summer (JJA: June, July, August) and autumn (SON: September, October, November).**
146 In case of spatially averaged trends, the **anomalies derived for the** individual station or
147 satellite pixel time series are first averaged in space and then the trends are calculated as
148 described above. The obtained trends for each dataset are then presented either in the
149 way of so-called Trendraster-plots or, in case of spatial trends, as spatial maps.

150 **The Trendraster-plot, or running trend analysis [Brunetti et al., 2006], is a way to**
151 **represent, in a condensed way, the trends for different subperiods with different lengths.**
152 **The advantage of the Trendraster-plots is that mid- and longer-term variability can be**
153 **compared easily. Specifically, the y-axis represents the starting year while the x-axis**
154 **represents the last year of the considered period. The color of each pixel shows the**
155 **intensity (linear trend $W/m^2/decade$) of the trend in the considered period**

156 In some cases 95%-confidence intervals of the linear trends are given. These confidence
157 intervals are used to analyse **wether** a trend is statistically significantly positive (nega-
158 tive), which is the case if both the lower and upper 95%-confidence interval are positive
159 (negative). Further, if the confidence intervals of **trends derived from** different data do
160 overlap, they can be considered **to be** not statistically different.

4. Evaluation of Accuracy

161 In this section a basic validation of the CLARA-A2 and SARA-2 climate data records
162 with reference to the 53 stations in Europe is presented. A prerequisite for satellite climate
163 data records be usable for climate purposes is to reasonably reproduce anomalies. Further
164 a **low** bias and **low** mean absolute deviations (MAD) **compared to reference measurements**
165 are desired.

166 Figure 2 shows the mean SSR based on the two CM SAF climate data records analysed in
167 this study. Both data records overall agree in the general structure of SSR for Europe. For
168 the CLARA-A2 climate data record, the limited **number of** observations during daylight
169 in wintertime **does** not allow the calculation of monthly means for latitudes higher than
170 about $55^{\circ}N$ **during the full year**. Subsequently the data is set to missing in the CLARA-
171 A2 climate data record of SSR for the corresponding area **during twilight situations**, as
172 can be observed in Figure 2.

173 The validation of the CLARA-A2 monthly solar radiation data with the station data re-
174 veals on average a negative bias of $-0.4 W/m^2$ and a MAD of $7.3 W/m^2$ (cf. Table 2). The
175 SARA-2 monthly SSR data has a positive bias of $+2.7 W/m^2$ and a MAD of $6.9 W/m^2$.
176 The correlation coefficient of monthly anomalies is 0.88 for CLARA-A2 and 0.89 for

177 SARAH-2, documenting that both data records are well suited for the monitoring of
178 monthly anomalies.

179 The scatterplots of the monthly anomalies derived from CLARA-A2 and SARAH-2
180 versus the station data are shown in Figure 3, where it is distinguished between the time
181 periods before and after 1992. In 1992, the temporal sampling of the CLARA-A2 cli-
182 mate data record is improved by the availability of a second AVHRR sensor [*Karlsson*
183 *et al.*, 2017b]. As shown in Figure 3 (bottom), the correlation of anomalies substantially
184 increased after 1991 from 0.848 to 0.904. For this reason, in the following analysis the first
185 10 years of the CLARA-A2 climate data record (1982-1991) are left out to ensure a high
186 temporal stability of the satellite data. Moreover, there are, depending on latitude, up to
187 50% missing data before 1991 in the CLARA-A2 SSR and as a consequence the absolute
188 bias for the early years increases to about $10 W/m^2$ for CLARA-A2, which is more than
189 30% higher than for the period after 1991 (see Table 2). The correlation of anomalies is
190 around 0.90 for both periods for the SARAH-2 climate data record (cf. Figure 3 allowing
191 the analysis of SARAH-2 for the full period of 1983-2015 in this study).

192 Overall the basic evaluation of the CM SAF CLARA-A2 and SARAH-2 climate data
193 records highlights their high quality and accuracy, which allows a detailed analysis of SSR
194 using these satellite-based climate data records provided by the CM SAF.

5. Trend and Variability Analysis

195 In this part, variability and trends of SSR derived from the CM SAF's SARAH-2 and
196 CLARA-A2 climate data records are evaluated using the station data. Further, the spatial
197 distribution of trends based on the satellite data records are shown.

198 The mean anomaly time series of SARA-2, CLARA-A2 and the stations for the 53
199 European locations are shown in Figure 4. It is thereby distinguished between the time
200 periods of 1983-2015 and 1992-2015 (as noted in Section 4). Figure 4 shows that the
201 time series of monthly anomalies agree well between the data records even though the
202 differences are larger in some periods, for example around 1990 between SARA-2 and
203 the station-based data. Possible reasons for these slightly larger differences are satellite
204 changes, the disregard of the aerosol radiative effect of the Pinatubo eruption in 1991, or
205 other unknown issues in either the satellite or the station data.

206 Regarding the linear trends, all three data records agree reasonably well for both the
207 longer and shorter time period (cf. Figure 4), **even though both SARA-2 and CLARA-**
208 **A2 use an aerosol climatology as input.** All data records **exhibit** positive trends in
209 SSR **between** 1.9 to $2.4 W/m^2/decade$ for the period 1983-2015, and **between** 2.7 to
210 $3.0 W/m^2/decade$ for the time period 1992-2015. The trends in the station data are
211 overall larger than in the satellite data, while the SARA-2 trends are somewhat closer
212 to those observed at the stations than **the trends derived from** CLARA-A2. As shown in
213 Figure 4, the mean trends do agree within their confidence intervals, as the intervals are
214 overlapping each other.

215 A way to analyze trends during different time periods is by using running trend analysis
216 as depicted by so-called Trendraster-plots. A Trendraster-plot for the 53 station mean SSR
217 and of the corresponding data of SARA-2 and CLARA-A2 (at the station locations) is
218 shown in Figure 5. All three Trendraster-plots of SARA-2, CLARA-A2 and the stations
219 agree in an overall brightening in Europe, shown by the red squares in the lower right
220 part of the Trendraster-plots, which represent the trends of the longest time periods.

221 Further there is not only a reasonable agreement in the overall positive trends, but
222 there is also agreement in the shorter-term trends, i.e. the decadal variability. In the
223 early years, from 1983 to the late 1990's there is a positive trend in SSR, which is followed
224 by a **zero** or slightly negative trend during the time period of the late 1980's until about
225 2002. From the mid 1990's to the mid 2000's the trends are positive again **with values**
226 **between $6-8 W/m^2/decade$ consistent between the data records**. During the latest years
227 (i.e. **after ~ 2006**) the SSR trends are small. The most positive trends are found in the
228 1990's in the CLARA-A2 climate data record with values of up to $+8 W/m^2/decade$. The
229 mainly **zero** (or slightly negative) trends of SSR during about 1989-2000 are smaller in
230 the SARA-2 climate data record **than those derived from** the station data.

231 The regional trends over the 33 year time period are shown in Figure 6. For each of
232 the 5 regions (c.f. Figure 1), a boxplot is used to **depict** the distribution of the linear
233 trends **for the locations** in the different regions. Each boxplot shows the **mean an the**
234 **median of the trends as well as quartiles, percentiles and outliers**. Figure 6 compares the
235 regional trends during the time period 1983-2015, when SARA-2 and the stations are
236 used, and during the shorter time period 1992-2015, when also CLARA-A2 is used. It
237 is shown that the mean regional trends are all positive and are mostly ranging between
238 2 and $4 W/m^2/decade$. In all regions, **except** the region South, the trends between the
239 two satellite climate data records and the stations agree well. An exception is found in
240 the region South, where the trends **based on** station data are much larger than in the
241 CMSAF's satellite climate data records, for both analyzed time periods. In the region
242 South, the mean trend **based on** the station data are in the order of 5 to $6 W/m^2/decade$,
243 while the trends based on SARA-2 and CLARA-A2 data are **consistently lower** in the

244 order of $2W/m^2/decade$. The larger spread in the trends among the stations in region
245 South is evident, in particular for the shorter time period (cf. outliers in Figure 6), **when**
246 **trends range from 3 to $10W/m^2/decade$.**

247 A worthwhile characteristic of satellite data is its provision of spatially complete infor-
248 mation. The spatial pattern of the linear trends of SSR in Europe given by the CMSAF
249 SARA-2 and CLARA-A2 are shown in Figure 7. For comparison the SSR trends of the
250 station data are added. In the left part of Figure 7 the trend of SARA-2 for the full
251 33-year period is shown. The largest positive trend is found in Eastern Europe (especially
252 east of the Carpathian Mountains). Strong positive trends of SSR are also visible in parts
253 of Central Europe and over the North and Baltic Sea. **Some regions experience a low or**
254 **negative trend** during the time period 1983-2015 e.g. parts of France and Great Britain.

255 Figure 7 also provides the SSR trends for the time period 1992-2015 for the CLARA-A2
256 and the SARA-2 data records. There is a remarkable agreement between both **data**
257 **records** in the mean trends at the stations (cf. Figure 4), and in its spatial pattern,
258 especially over land. **During the time period 1992-2015 the** most positive trends can be
259 found in Eastern Europe while slightly negative trends **are derived** in parts of the Eastern
260 Mediterranean region in both data records. Over the oceans, especially over the Atlantic
261 Ocean and the North Sea, the trends are more positive in the CLARA-A2 climate data
262 record than in the SARA-2 climate data record. The CLARA-A2 SSR also has a more
263 **distinct** land-ocean difference in trends compared to the SARA-2 SSR.

264 The mean **seasonal** trends of SSR **for the five regions** are shown in Figure 8. In all
265 regions, **except** in the region South, the strongest positive trends in SSR are observed in
266 the spring season, with values in the range of about 4 to $6W/m^2/decade$. In summer,

267 the trends are also positive, with extreme positive trends given by the station data in the
268 region South, where the mean trend is around $9 W/m^2/decade$, in line with results from
269 *Sanchez-Lorenzo et al.* [2015] and *Manara et al.* [2016]. Again we find an overall tendency
270 of a slight underestimation of the positive trends of the satellite data with reference to
271 the station data, mainly in spring and summer. Based on the sign and magnitude of the
272 SSR trends(cf. Figure 8), we conclude that there is a reasonable agreement between the
273 CMSAF's satellite and the station data. Notable exception it the region South during
274 summer, which will be discussed in more detail in Section 5.2.

275 Similar to the trend over the 33-years time period shown in Figure 8, Figure 9 presents
276 the regional and seasonal trends for the shorter time period of 1992-2015, for which the
277 CLARA-A2 climate data record is analysed as well. We find larger differences in the trends
278 of the different data records for the shorter time period. As expected, the absolute trends
279 in the different regions and seasons are partly different to the ones derived for the 33-year
280 time period (Figure 8). For example, in the region Central-West, the strongest positive
281 trends between 1992 and 2015 occur in autumn and not in spring. Again, disagreements
282 in the trends are obvious in the region South. Especially during the summer season, the
283 station data show strong positive trends of more than $10 W/m^2/decade$ (see dot at the top
284 of Figure 9), while the satellite-based data indicate trends of about 3 to $4 W/m^2/decade$.
285 Figure 9 also shows that there are some negative trends for the time period 1992-2015,
286 e.g. in the region North's winter season. Still, the trends in the majority of regions and
287 seasons are positive, documenting the general increase of SSR. There is a good agreement
288 between the three data records in the regions Central-East, Central-West and North-West,
289 while differences are larger in the regions South and North.

290 The spatial distribution of the seasonal trends in SSR based on the CMSAF's climate
291 data records are shown in Figure 10 and 11. In Figure 10, the trends based on SARA-2
292 and the station data are shown for the time period 1983-2015. It is obvious that there
293 are large differences between the trends in the different seasons. The smallest trends
294 (negative in some regions like Eastern Europe) are observed in winter while the largest
295 ones are observed in spring (c.f. Figure 10, top right) when in large areas of Central and
296 Eastern Europe the trends exceed $5 W/m^2/decade$. In summer, the trends remain positive
297 in the East, but some areas in the West, namely parts of France and Great Britain show
298 slightly negative trends, in line with the station data (c.f. Figure 10, bottom left). In
299 autumn, there are small positive trends in most of Europe, while the trends are mainly
300 negative in the South East of Europe. These negative trends in autumn (i.e. in the Balkan
301 states) have also been found by *Alexandri et al.* [2017] for the time period 1983-2013.

302 To compare the trends derived from SARA-2 and CLARA-A2, the spatial trend maps
303 are shown in Figure 11 for the common time period of 1992-2015. The Figure 11 reveals
304 similar spatial patterns of seasonal trends in Europe of SARA-2 and CLARA-A2, which
305 indicates a consistency of the independently derived climate data records. It should
306 be noted that the overall agreement in the trends between the satellite and stations
307 data is also valid for the individual stations (with the exception of region South). By
308 comparing the seasonal trend patterns given by Figure 10 and 11, it is visible that the
309 spatial variability of trends in Europe is large, especially on shorter time scales. In general,
310 it has been found that the trends can substantially vary, even if the time period considered
311 is only slightly changed.

312 Motivated by the results shown in Figure 8 and 9, we present additional analysis for the
313 regions North and South in the following sections.

5.1. Focus: Region North

314 In the region North the trends derived from the satellite-based data records and the
315 from the station data agree in spring and autumn in the region North, but there are larger
316 differences in the summer and winter season, in particular during the time period 1992-
317 2015 (as shown in Figure 9). In this period, during the summer season, both SARA-2
318 and CLARA-A2 have negative trends of -1 to $-2 W/m^2/decade$ while the station data
319 has a positive trend of 2 to $3 W/m^2/decade$. In the winter season the differences are
320 the opposite with positive values for SARA-2 and negative trends based on the station
321 data (no CLARA-A2 data analyzed here due to missing data). However, for the full time
322 period of 1983-2015, the trends of SSR agree (cf. Figure 8).

323 To further investigate these differences between the trends the Trendraster-plots for
324 region North are shown for the winter and summer season for both the station data and
325 SARA-2 (cf. Figure 12). In winter, it is visible that even though the long term trend
326 agrees (no trend during the period 1983-2015), there are substantial differences on the
327 shorter term (cf. Figure 12, upper part). Most obvious are the relatively strong positive
328 trends during the winter season in the SARA-2 data starting in mid 1990's onwards.
329 During that period, SARA-2 shows a larger positive trend in SSR than the surface
330 observations. Relative trends can reach up to $+15\%$ SSR per decade, which is due to the
331 low absolute values SSR levels in winter. One possible reason for the trend overestimation
332 by SARA-2 is related to the fact that snow on the ground can be misinterpreted as
333 clouds in the satellite retrieval scheme used in the generation of SARA-2 resulting in

334 an underestimation of SSR under snow-covered conditions. A change in the snow cover
335 would result in an artificial change in SSR in the SARA-2 climate data record, because
336 the underestimation of SSR under snow-covered conditions would be reduced. Hence the
337 negative trend in snow cover during the mid 1990's in the region North [*Brown et al.*, 2011],
338 might have contributed to the positive trend in the SARA-2 data record in wintertime
339 SSR in the region North. Nevertheless, it should be noted that a slight positive trend is
340 also observed also by the stations during that time period even if it is smaller compared
341 to SARA-2. However, at this stage we cannot rule out an impact of the change in the
342 satellite instruments used in the generation of SARA-2 in 2006 on the differences in the
343 trends we are finding in the region North in winter.

344 During the summer, the trends are higher than during the winter, and the trend is
345 overall positive in both the station data and the SARA-2 data (cf. Figure 12, lower
346 part). The temporal variability of the trends is high in both data records. The SARA-
347 2-based trends ending after 2007 tend to be smaller than the trends based on station data.
348 Possible reasons are a change in the onset of snow coverage or an inhomogeneity from the
349 change in the satellite instruments.

350 Overall we conclude that the trends based on satellite data in the region North need to
351 be considered with care. The study of *Riihelä et al.* [2015] finds a good correspondence
352 between satellite- and station-based trends, but did not assess seasonal trends, where the
353 larger differences appear in the present study.

5.2. Focus: Region South

354 The region South exhibits the largest differences in trends between the satellite climate
355 data records and the station data (cf. Figures 6,8,9). To get more insights, additional

356 Trendraster-plots based on SARA-2, CLARA-A2 and the station data for the region
357 South are presented in Figure 13 for all seasons. In winter, spring and autumn, there is a
358 general agreement between the satellite data and the station data, even though there is a
359 small tendency of the satellite data to underestimate the trends in SSR with reference to
360 the station data. For the common time period of 1992-2015, the SARA-2 Trendrasters
361 compared better with the station-based Trendraster than the CLARA-A2 Trendrasters.

362 The largest differences are evident in the summer season (see Figure 13, third row),
363 where SARA-2 and CLARA-2 clearly disagree with the station data. In fact, the satellite
364 data show a much smaller positive trend than the station data. It is remarkable, that
365 SARA-2 and CLARA-A2 agree well for the summer season with each other, even though
366 they are based on different sensors on different satellites and so they are independent.

367 However, there is one relevant aspect that both SARA-2 and CLARA-A2 have in com-
368 mon: the use of a constant monthly climatology of aerosol information as input [*Müller et*
369 *al.*, 2015 b]. A decreasing aerosol load, as for example reported in Spain [*Sanchez-Romero*
370 *et al.*, 2016] or over the mainland Europe [*Ruckstuhl et al.*, 2008] since the 1980s would
371 lead to a positive trend in SSR, due to the reduced direct aerosol effect on SSR, which
372 would not be captured by SARA-2 or CLARA-A2. This fact might be one explanation
373 of the underestimation of the trend by both SARA-2 and CLARA-A2 with reference to
374 the station data. This hypothesis seems to be confirmed also considering recent results
375 published by *Georgoulas et al.* [2016b]. They investigated the spatio-temporal evolution
376 (since 2000s) of the aerosol optical depth over the greater Mediterranean Region finding
377 that the sub-regions with the stronger negative Aerosol Optical Density (AOD550) trend
378 are the Central Mediterranean and the Iberian Peninsula, attributed to the positive pre-

379 cipitation trends all over the region and to the decrease of anthropogenic emissions in the
380 area.

381 On the other hand, the major part of the variability and trends in Europe are reasonably
382 captured by the CM SAF's SARA-H-2 and CLARA-A2 climate data records, including the
383 region Central-East. The region South's summer season is an exception in this respect.
384 However, it should be considered that in this region, the SSR is likely being more affected
385 by potential changes of the aerosol direct effect [*Nabat et al.*, 2014], as clear-sky days
386 are more frequent in the Mediterranean summer than in other European areas. This is
387 coherent with the findings of *Kambezidis et al.* [2016], who found higher values under
388 clean skies (without aerosols but including clouds) compared to those under clear skies
389 (without clouds but including aerosols) using reanalysis data of surface net shortwave
390 radiation during June-August, indicating that aerosols attenuate more the shortwave ra-
391 diation compared to clouds over the Mediterranean in summer. Moreover, a positive
392 trend in clear-sky SSR in Europe has been found by *Bartók* [2017] during the time period
393 2001-2012, which is partly attributed to a reduced aerosol load. This signal is confirmed
394 both by *Manara et al.* [2016] for the Italian territory and by *Sanchez-Lorenzo and Wild*
395 [2012] over Switzerland. The former found during the brightening period stronger positive
396 SSR tendencies under clear-sky conditions than under all-sky conditions suggesting that
397 cloud cover variations have partially masked the variations caused by aerosols variations
398 (both anthropogenic and natural) especially during winter and autumn. The latter found
399 in the clear sky SSR series during the sub-period 1981-2010 a positive trend especially in
400 spring and summer attributing them to the direct aerosol effect [*Ruckstuhl et al.*, 2008;
401 *Ruckstuhl and Norris* 2009].

402 While the neglect of the change in the aerosol loading is the satellite retrieval provide
403 a possible and likely reason for the underestimation of the trend by the satellite data
404 sets, the impact of the change in the instrumentation to measure the SSR at the surface
405 stations has not yet been quantified and a possible impact on the trend calculation based
406 on station data cannot be ruled out at this stage.

6. Discussion and Conclusions

407 In this study, the variability and trends of surface solar radiation are analyzed in Eu-
408 rope during the time period 1983-2015. Here, the CMSAF's SARA-2 and CLARA-A2
409 climate data records of SSR are compared to surface observations to assess their ability to
410 reproduce the surface observations. It is found that the overall variability and the trends
411 agree well between the CMSAF's SARA-2, CLARA-A2 and the station data in Europe.
412 It is important to mention that the CLARA-A2 and the SARA-2 data records are inde-
413 pendent from each other, as they are based on different satellite systems and algorithms.
414 So, the agreement in trends and variability (especially over the continent) for the time
415 period for which both data records are used (1992-2015) is remarkable and documents the
416 high quality of SARA-2 and CLARA-A2 (see e.g. Figures 7 and 11). Possible reasons
417 for the remaining differences between the SSR trends in the satellite and station data
418 might be connected to the neglect of changes in the aerosol loading [e.g. Bartók, 2017;
419 Sanchez-Lorenzo et al., 2017] and to effects of a change in snow cover, as described in
420 section 5.1. It is important to mention that the clear-sky radiation given by SARA-2
421 (and CLARA-A2), which are only driven by the time varying water vapor input, do show
422 negligible trends of SSR of mostly below $\pm 0.2 W/m^2/decade$ (not shown), consistent
423 with previous results [Posselt et al., 2014]. The largest negative trends in the SARA-2

424 clear-sky radiation are found the Balkan region and in South Eastern Europe with up to
425 $-0.6 W/m^2/decade$, which is still much smaller than most of the all-sky SSR trends.

426 The CMSAF's SARA-H-2 and CLARA-A2 have reached a high quality and stability,
427 that enables the analysis of variability and trends in SSR. The observed positive trends of
428 SSR (considering both the satellite data records and the station data) are about 1.9 to 2.4
429 $W/m^2/decade$. Stronger positive trends of about 2.7 to 3.0 $W/m^2/decade$ are observed
430 during the shorter time period of 1992-2015 (cf. Figure 4). Figure 5 shows that also the
431 variability of SSR agrees between the CMSAF's satellite climate data records and the
432 station data. The spatial view on the long-term SSR trends reveal that the strongest
433 brightening is found for the spring season, and mainly in Eastern Europe and in the
434 North Western Europe (cf. Figures 7 and 10). Overall the spatial trend patterns and
435 its seasonal variability are similar to findings by *Sanchez-Lorenzo et al.* [2017] over the
436 1983-2010 period. An exception is seen for the summer season in region South, where the
437 trends based on the satellite data records and the station data disagree (cf. Figure 8).
438 There, the positive trend observed by the station data is underestimated by the satellite
439 data (cf. Section 5.2). However, the spread between the trends in the station data is also
440 largest in the region South (cf. Figure 6), which indicates that regional to local causes for
441 trends might potentially exist as well. In general, even though care has been taken in the
442 data compilation, remaining data inhomogeneities (e.g. due to instrumental changes) in
443 either satellite or stations data can not be fully excluded.

444 Aerosol information is kept constant for both SARA-H-2 and CLARA-A2, because of the
445 non-availability of high quality aerosol information for the full time period of the satellite
446 data at the time of data generation [*Müller et al.*, 2015 b]. It is important to note, that,

447 even though the aerosol information is kept constant within SARA-H-2 and CLARA-A2,
448 changes of the aerosol indirect effect is expected to be captured [Müller *et al.*, 2015 b], i.e.
449 through the changes in cloud brightness and life time.

450 The Mediterranean region is affected by large aerosol loads for anthropogenic and natu-
451 ral reasons. It is affected by sea salt aerosols from the Mediterranean Sea and the Atlantic
452 Ocean, pollution aerosols from Europe, dust from the Sahara desert and biomass burn-
453 ing aerosols from Eastern Europe. Moreover, depending on the season, different types of
454 aerosols reach different parts of the region (e.g., dust peaks in spring over the Eastern
455 Mediterranean, in summer over the Western Mediterranean and in spring and summer
456 over the transitional region of Central Mediterranean) [Georgoulas *et al.*, 2016a, b; Floutsis
457 *et al.*, 2016; Kanakidou *et al.*, 2011; Lelieveld *et al.*, 2002]. For this reason, the influence
458 of the aerosol direct effect on SSR is supposed to be large in the region South [Bartók,
459 2017; Sanchez-Lorenzo *et al.*, 2017; Kambezidis *et al.*, 2016; Nabat *et al.*, 2014]. This al-
460 lows to conclude that at least parts of the differences between satellite and station data
461 found in the region South’s summer (cf. section 5.2) might be attributed to the missing
462 of changes in the aerosol direct effect in the satellite data records [Sanchez-Lorenzo *et*
463 *al.*, 2017]. Sanchez-Lorenzo *et al.* [2017] also found, for a shorter time period, that for
464 the majority of Europe the differences in trends between the satellite-based SSR data and
465 station data were small, even though a constant aerosol approach [Posselt *et al.*, 2012] has
466 been used in generating the satellite data record, which is overall in line with the findings
467 of this study. For the time period since the 2000s Mateos *et al.* [2014] states that over the
468 Iberian Peninsula three fourths of the SSR trend is explained by changes in clouds.

469 Another peculiarity is found in the region North, where the running-trend analysis re-
470 vealed that for the time period from the mid 1990's onwards, the trends are overestimated
471 by the SARA-2 climate data record with reference to the station data. As noted in sec-
472 tion 5.1, a reduction in snow cover could potentially lead to a positive trend in SSR in the
473 satellite data records.

474 However, for the other regions in Europe, the trends and variability of SSR between
475 satellite and station data agree reasonably well for all seasons, which **suggests** that aerosol
476 changes (especially aerosol direct effects) play **only** a minor role for the observed trends in
477 SSR in these regions. Further, based on the algorithms and their input used to generate
478 the SARA-2 and CLARA-A2 climate data records [cf. *Müller et al.*, 2015; *Karlsson*
479 *et al.*, 2017b], and based on an analysis of trends in water vapor, which is found to be
480 negligible, it can be concluded, that the large majority of the observed positive trends
481 in SSR in Europe are due to changes in clouds. This finding is also **consistent with the**
482 **results of Sanchez-Lozeno 2017, based on satellite- and surface-based cloud data records,**
483 **including the first version of the CLARA data record, who found a decrease in cloud**
484 **coverage in Europe. The results are robust when using the CLARA-A2 data record (not**
485 **shown).**

486 In general, the changes in cloud radiative effects reproduced by SARA-2 and CLARA-
487 A2 can be due to natural cloud variability and/or changes in the aerosol effects on clouds,
488 and consequently aerosol effects can not be ruled out completely through indirect aerosol
489 effects. Nevertheless, it is worth noting that at present most of the literature using
490 ground-based data or climate model simulations have reported that the major cause of
491 the brightening in Europe, especially in Central Europe, is related to the direct aerosol

492 effects via a decrease in anthropogenic aerosol emissions since the 1980s [e.g. *Norris and*
493 *Wild*, 2007; *Philipona et al.*, 2009; *Zubler et al.*, 2011; *Nabat et al.*, 2014]. *Boers et al.*
494 [2017] found that positive trends in SSR in the Netherlands are due to changes in both
495 aerosols and clouds.

496 Consequently, the results of this study add new information to the available literature.
497 Also in some previous studies the dimming period observed between the 1950s and 1980s
498 was mainly attributed to cloud changes instead of direct aerosol effects [*Liepert*, 1997].
499 *Stjern et al.* [2009] and *Parding et al.* [2016] also found that changes in clouds are the
500 main reason for trends in SSR in Northern Europe, and in the Mediterranean observations
501 indicate fewer clouds for the period 1971 to 2005 [*Sanchez-Lorenzo et al.*, 2017b]. In the
502 United States, observed positive trends in SSR since the 1990s are also mainly attributed
503 to changes in cloud cover [*Augustine et al.*, 2013].

504 While it can be assumed that the quality of the satellite-based data records as docu-
505 mented here is representative also for other regions available in the satellite data record,
506 a comparison with high-quality surface data is always recommended when possible. Since
507 no reliable data are available for large parts of th world satellite data will remain the only
508 observational source of climatic information.

509 In any case, further research is needed to consolidate the reasons and the mechanisms
510 behind the variability and trends in SSR since the 1980s in Europe. This study documents
511 the quality of the satellite-derived data records to help addressing those topics in future
512 studies and investigations. In particular the capturing of the spatial structure of the
513 trends in SSR might help to identify the relevant processes.

514 **Acknowledgments.**

515 The used EUMETSAT CMSAF's SARAH-2 and CLARA-A2 climate data records are
516 freely available via <http://www.cmsaf.eu/wui>. The majority of station data used (except
517 for some Spanish and Italian stations) can be obtained from the GEBA archive via [http:
518 //www.geba.ethz.ch/](http://www.geba.ethz.ch/). The authors thank the data providers for free data access. ASL
519 was supported by a postdoctorial fellowship JCI-2012-12508 and the projects CGL2014-
520 55976-R and CGL2014-52135-C3-1-R funded by the Spanish Ministry of Economy and
521 Competitiveness.

References

- 522 Alexandri, G., Georgoulas, A.K., Meleti, C., Balis, D., Kourtidis, K.A., Sanchez-Lorenzo,
523 A., Trentmann, J. and Panis, P. (2017), A high resolution satellite view of surface solar
524 radiation over the climatically sensitive region of Eastern Mediterranean, *Atmospheric
525 Research*, *188*, 107–121, doi:10.1016/j.atmosres.2016.12.015.
- 526 Augustine, J. A. and Dutton, E. G. (2013), Variability of the surface radiation budget over
527 the United States from 1966 through 2011 from high-quality measurements, *Journal of
528 Geophysical Research*, *188*, 1–11, doi:10.1029/2012JD018551.
- 529 Bartók, B. (2017), Aerosol radiative effects under clear skies over Europe and their changes
530 in the period of 2001–2012, *International Journal of Climatology*, *37(4)*, 1901–1909, doi:
531 10.1002/joc.4821.
- 532 Boers, R., Brandsma, T. and Siebesma, A. P. (2017), Impact of aerosol and clouds on
533 decadal trends in all-sky solar radiation over the Netherlands (1966-2015), *Atmospheric
534 Chemistry and Physics*, *17*, 8081–8100, doi:10.5194/acp-17-8081-2017.

535 Brown, R. D. and Robinson D. A. (2011), Northern Hemisphere spring snow cover variabil-
536 ity and change over 1922-2010 including an assessment of uncertainty, *The Cryosphere*,
537 5, 219–229, doi:10.5194/tc-5-219-2011.

538 Brunetti, M., Maugeri, M., Nanni, T., Auer, I., Böhm, R., Schöner, W. (2006), Pre-
539 cipitation variability and changes in the greater Alpine region over the 1800-2003 pe-
540 riod, *Journal of Geophysical Research - Atmosphere*, 111, D11107, 2156–2202, doi:
541 10.1029/2005JD00667.

542 Floutsi, A.A., Korras-Carraca, M.B., Matsoukas, C., Hatzianastassiou, N. and Biskos, G.
543 (2016), Climatology and trends of aerosol optical depth over the Mediterranean basin
544 during the last 12 years (2002-2014) based on Collection 006 MODIS-Aqua data, *Science*
545 *of The Total Environment*, 551552, 292–303, ISSN 0048-9697, doi:10.1016/j.scitotenv.
546 2016.01.192.

547 Georgoulias, A. K., Alexandri, G., Kourtidis, K. A., Lelieveld, J., Zanis, P., Pschl, U.,
548 Levy, R., Amiridis, V., Marinou, E. and Tsikerdekis, A. (2016), Spatiotemporal vari-
549 ability and contribution of different aerosol types to the aerosol optical depth over
550 the Eastern Mediterranean, *Atmospheric Chemistry and Physics*, 16, 13853–13884, doi:
551 10.5194/acp-16-13853-2016.

552 Georgoulias, A. K., Alexandri, G., Kourtidis, K. A., Lelieveld, J., Zanis, P. and Amiridis,
553 V. (2016), Differences between the MODIS Collection 6 and 5.1 aerosol datasets over the
554 greater Mediterranean region, *Atmospheric Environment*, 147, 310–319, doi:10.1016/j.
555 atmosenv.2016.10.014.

556 Gilgen, H., Roesch, A., Wild, M. and Ohmura, A. (2009), Decadal changes in shortwave
557 irradiance at the surface in the period 1960 to 2000 estimated from Global Energy

558 Budget Archive Data, *Journal of Geophysical Research*, *114*, D00D08, doi:10.1029/
559 2008JD011383.

560 Hartmann, D. L., Ramanathan, V., Berroir, A. and Hunt, G. E. (1986), Earth Radiation
561 Budget data and climate research, *Reviews of Geophysics*, *24(2)*, 1944–9208, doi:10.
562 1029/RG024i002p00439.

563 Hinkelmann, L. M., Stackhouse Jr., P. W., Wielicki, B. A., Zhang, T. and Wilson, S. R.
564 (2009), Surface insolation trends from satellite and ground measurements: Comparisons
565 and challenges, *Journal of Geophysical Research - Atmospheres*, *114(D10)*, doi:10.1029/
566 2008JD011004.

567 Huld, T., Moner-Girona, M. and Kriston, A. (2017), Geospatial Analysis of Photovoltaic
568 Mini-Grid System Performance, *energies*, *10(218)*, doi:10.3390/en10020218.

569 Kambezidis, H.D., Kaskaoutis, D.G., Kalliampakos, G.K., Rashki A. and Wild M. (2016),
570 The solar dimming/brightening effect over the Mediterranean Basin in the period
571 19792012, *Journal of Atmospheric and Solar-Terrestrial Physics*, *150151*, 31–46, ISSN
572 1364-6826, doi:doi.org/10.1016/j.jastp.2016.10.006.

573 Kanakidou, M., Mihalopoulos, N., Kindap, T., Im, U., Vrekoussis, M., Gerasopoulos,
574 E., Dermizaki, E., Unal, A., Koak, M., Markakis, K., Melas, D., Kouvarakis, G.,
575 Youssef, A. F., Richter, A., Hatzianastassiou, N., Hilboll, A., Ebojie, F., Wittrock,
576 F., von Savigny, C., Burrows, J. P., Ladstaetter-Weissenmayer, A., and Moubasher, H.
577 (2011), Megacities as hot spots of air pollution in the East Mediterranean, *Atmospheric*
578 *Environment*, *45*, 1223–1235, doi:10.1016/j.atmosenv.2010.11.048.

579 Karlsson, K.-G., Anttila, K., Trentmann, J., Stengel, M., Fokke Meirink, J., Devasthale,
580 A., Hanschmann, T., Kothe, S., Jääskeläinen, E., Sedlar, J., Benas, N., van Zadelhoff,

581 G.-J., Schlundt, C., Stein, D., Finkensieper, S., Håkansson, N. and Hollmann, R., Fuchs,
582 P. and Werscheck, M. (2017a), CLARA-A2: CM SAF cLoud, Albedo and surface RA-
583 diation dataset from AVHRR data - Edition 2, Satellite Application Facility on Climate
584 Monitoring, doi:10.5676/EUM_SAF_CM/CLARA_AVHRR/V002

585 Karlsson, K.-G., Anttila, K., Trentmann, J., Stengel, M., Fokke Meirink, J., Devasthale,
586 A., Hanschmann, T., Kothe, S., Jääskeläinen, E., Sedlar, J., Benas, N., van Zadel-
587 hoff, G.-J., Schlundt, C., Stein, D., Finkensieper, S., Håkansson, N. and Hollmann,
588 R. (2017b), CLARA-A2: the second edition of the CM SAF cloud and radiation data
589 record from 34 years of global AVHRR data, *Atmospheric Chemistry and Physics*, 17(9),
590 doi:10.5194/acp-17-5809-2017.

591 Kothe, S., Pfeifroth, U., Cremer, R., Trentmann, J. and Hollmann R. (2017), A Satellite-
592 Based Sunshine Duration Climate Data Record for Europe and Africa, *Remote Sensing*,
593 9, 429, doi:10.3390/rs9050429.

594 Lelieveld, J., and coauthors (2002), Global Air Pollution Crossroads ober the Mediter-
595 ranean, *Science*, 298(5594), 794–799, doi:10.1126/science.1075457.

596 Liepert, B., Fabian, P. and Grassl, H. (1994), Solar radiation in Germany - observed
597 trends and an assessment of their causes Pt 1., *Contributions to Atmospheric Physics*,
598 67(1), 15–29.

599 Liepert, B. (1997), Recent changes in solar radiation under cloudy conditions in Germany,
600 *International Journal of Climatology*, 17(14), 1581–1593.

601 Manara, V., Brunetti, M., Celozzi, A., Maugeri, M., Sanchez-Lorenzo, A. and Wild, M.
602 (2016), Detection of dimming/brightening in Italy from homogenized all-sky and clear-
603 sky surface solar radiation records and underlying causes (1959-2013), *Atmospheric*

- 604 *Chemistry and Physics*, 16, 11145–11161, doi:10.5194/acp-16-11145-2016.
- 605 Mercado, L. M., Bellouin, N., Sitch, S., Boucher, O., Huntingford, C., Wild, M. and Cox,
606 P. M. (2009), Impacts of changes in diffuse radiation on the global land carbon sink,
607 *Nature*, 458, 1014–1087.
- 608 Miglietta, M.M., Huld, T. and Monforti-Ferrario F. (2017), Local Complementarity of
609 Wind and Solar Energy Resources over Europe: An Assessment Study from a Mete-
610 orological Perspective, *Journal of Applied Meteorology and Climatology*, 56,217–234,
611 doi:10.1175/JAMC-D-16-0031.1.
- 612 Müller, R., Pfeifroth, U., Traeger-Chattejee, C., Trentmann, J. and Cremer, R. (2015),
613 Digging the METEOSAT Treasure-3 Decades of Solar Surface Radiation, *Remote Sens-*
614 *ing*, 7(6), 8067–8101, doi:10.3390/rs70608067.
- 615 Müller, R., Pfeifroth, U. and Traeger-Chattejee, C. (2015), Towards Optimal Aerosol
616 Information for the Retrieval of Solar Surface Radiation Using Heliosat, *Atmosphere*, 6,
617 863–878, doi:10.3390/atmos6070863.
- 618 Ohmura, A. and Gilgen, H. (1993), Re-Evaluation of the Global Energy Balance, *Interac-*
619 *tions Between Global Climate Subsystems the Legacy of Hann (eds G.A. McBean and M.*
620 *Hantel)*, American Geophysical Union, Washington, D. C., doi:10.1029/GM075p0093.
- 621 Ohmura, A., Dutton, E. G., Forgan, B., Frohlich, C., Gilgen, H., Hegner, H., Heimo, A.,
622 König-Langlo, G., McArthur, B., Muller, G., Philipona, R., Pinker, R., Whitlock, C. H.,
623 Dehne, K. and Wild, M. (1998), Baseline Surface Radiation Network (BSRN/WCRP):
624 New precision radiometry for climate research, *Bulletin of the American Meteorolog-*
625 *ical Society*, 79, 2115–2136, doi:10.1175/1520-0477(1998)079\textless2115:BSRNBW\
626 \textgreater;2.0.CO;2.

- 627 Ohmura, A. (2009), Observed decadal variations in surface solar radiation and their
628 causes, *Journal of Geophysical Research*, *114*, D00D05, doi:10.1029/2008JD011290.
- 629 Mateos, D., Sanchez-Lorenzo, A., Antón, M., Cachorro, V. E., Calbó J., Costa, M. J.,
630 Torres, B. and Wild, M. (2014), Quantifying the respective roles of aerosols and clouds
631 in the strong brightening since the early 2000s over the Iberian Peninsula, *Journal of*
632 *Geophysical Research: Atmospheres*, *119*, 10382–10393, doi:10.1002/2014JD022076.
- 633 Nabat, P., Somot, S., Mallet, M., Sanchez-Lorenzo, A. and Wild, M. (2014), Contribution
634 of anthropogenic sulfate aerosols to the changing Euro-Mediterranean climate since
635 1980, *Geophysical Research Letters*, *41(15)*, 5605–5611, doi:10.1002/2014GL060798.
- 636 Norris, J. R., Wild, M. (2014), Trends in aerosol radiative effects over Europe inferred
637 from observed cloud cover, solar dimming, and solar brightening, *Journal of Geophysical*
638 *Research*, *112(D08214)*, doi:10.1029/2006JD007794.
- 639 Parding, K. M., Liepert, B. G., Hinkelmann, L. M., Ackerman, T. P., Dagestad, K.-
640 F. and Olseth, J. A. (2016), Influence of Synoptic Weather Patterns on Solar ir-
641 radiance Variability in Northern Europe, *Journal of Climate*, *29*, 4229–4250, doi:
642 10.1175/JCLI-D-15-0476.1.
- 643 Pfeifroth, U., Kothe, S., Müller, R., Trentmann, J., Hollmann, R., Fuchs, P. and Wer-
644 scheck, M (2017), Surface Radiation Data Set - Heliosat (SARAH) - Edition 2, Satel-
645 lite Application Facility on Climate Monitoring, doi:10.5676/EUM.SAF_CM/SARAH/
646 V002.
- 647 Philipona, R., Behrens, K. and Ruckstuhl, C. (2009), How declining aerosols and rising
648 greenhouse gases forced rapid warming in Europe since the 1980s, *Geophysical Research*
649 *Letters*, *36(L02806)*, doi:10.1029/2008GL036350.

- 650 Posselt, R., Müller, R. W., Stöckli, R. and Trentmann, J. (2012), Remote sensing of solar
651 surface radiation for climate monitoring – the CM-SAF retrieval in international com-
652 parison, *Remote Sensing of Environment*, *118*, 186–198, doi:10.1016/j.rse.2011.11.016.
- 653
- 654 Posselt, R., Müller, R., Trentmann, J., Stöckli, R. and Liniger, M. A. (2014), A surface
655 radiation climatology across two Meteosat satellite generations, *Remote Sensing of En-
656 vironment*, *142*, 103–110, doi:10.1016/j.rse.2013.11.007.
- 657 Ramanathan, V., Crutzen, P. J., Kiehl, J. T. and Rosenfeld, D. (2001), Aerosols, Cli-
658 mate, and the Hydrological Cycle, *Science*, *294(5549)*, 2119–2124, doi:10.1126/science.
659 1064034.
- 660 Raschke, E., Kinne, S., Rossow, W. B., Stackhouse Jr., P. W. and Wild, M. (2016),
661 Comparison of Radiative Energy Flows in Observational Datasets and Climate Mod-
662 eling, *Journal of Applied Meteorology and Climatology*, *55*, 93–117, doi:10.1175/
663 JAMC-D-14-0281.1.
- 664 Riihelä, A., Carlund, T., Trentmann, J., Müller, R. and Lindfors A. V.(2015), Validation
665 of CM SAF Surface Solar Radiation Datasets over Finland and Sweden, *Remote Sensing*,
666 *7(6)*, 6663–6682, doi:10.3390/rs70606663.
- 667 Ruckstuhl C., and coauthors (2008), Aerosol and cloud effects on solar brighten-
668 ing and the recent rapid warming, *Geophysical Research Letters*, *35*, L12708, doi:
669 10.1029/2008GL034228.
- 670 Sanchez-Lorenzo A. and Wild M. (2012), Decadal variations in estimated surface solar
671 radiation over Switzerland since the late 19th century, *Atmospheric Chemistry and
672 Physics*, *12*, 8635–8644, doi:10.5194/acp-12-8635-2012.

- 673 Sanchez-Lorenzo A., Calbó J. and Wild M. (2013), Global and diffuse solar radiation in
674 Spain: Building a homogeneous dataset and assessing their trends, *Global and Planetary*
675 *Change*, *100(18)*, 343–352, doi:10.1016/j.gloplacha.2012.11.010.
- 676 Sanchez-Lorenzo, A., Wild, M., Brunetti, M., Guijarro, J. A., Hakuba, M. Z., Calbó, J.,
677 Mystakidis, S. and Bartók, B. (2015), Reassessment and update of long-term trends in
678 downward surface shortwave radiation over Europe (1939–2012), *Journal of Geophysical*
679 *Research: Atmospheres*, *120(18)*, 2169–8996, doi:10.1002/2015JD023321.
- 680 Sanchez-Lorenzo, A., Enriquez-Alonso, A., Wild, M., Trentmann, J., Vincente-Serrano,
681 S. M., Sanchez-Romero, A., Posselt, R. and Hakuba, M. (2017), Trends in downward
682 surface solar radiation from satellites and ground observations over Europe during 1983–
683 2010, *Remote Sensing of the Environment*, *189*, 108–117, doi:10.1016/j.rse.2016.11.018.
- 684 Sanchez-Lorenzo, A., Enriquez-Alonso, A., Calbó, J., González, J.-A., Wild, M., Follini,
685 D., Norris, J. R. and Vincente-Serrano, S. M. (2017), Fewer clouds in the Mediterranean:
686 consistency of observations and climate simulations, *Scientific Reports*, *7*, 41475, doi:
687 10.1038/srep41475.
- 688 Sanchez-Romero, A., Sanchez-Lorenzo, A., Gonzáles, J.A. and Calbó, J. (2016), Recon-
689 struction of long-term aerosol optical depth series with sunshine duration records, *Geo-*
690 *physical Research Letters*, *43(3)*, 1296–1305, doi:10.1002/2015GL067543.
- 691 Schulz J., and coauthors (2009), Operational climate monitoring from space: the EU-
692 METSAT Satellite Application Facility on Climate Monitoring (CM-SAF), *Atmospheric*
693 *Chemistry and Physics*, *9*, 1687–1709.
- 694 Stanhill G. (1983), The distribution of global solar radiation over the land surfaces of the
695 earth, *Solar Energy*, *31(1)*, 95–104, doi:10.1016/0038-092X(83)90039-7.

- 696 Stanhill, G. and Cohen, S. (2001), Global Dimming: A Review of the Evidence for a
697 Widespread and Significant Reduction in Global Radiation with Discussion of Its Prob-
698 able Causes and Possible Agricultural Consequences, *Agricultural and Forest Meteorol-*
699 *ogy*, *107*, 255–278, doi:http://dx.doi.org/10.1016/S0168-1923(00)00241-0.
- 700 Stjern, C. W., Kristjánsson, J. E. and Hansen, A. W. (2009), Global dimming and global
701 brightening an analysis of surface radiation and cloud cover data in northern Europe,
702 *International Journal of Climatology*, *29(5)*, 643–653, doi:10.1002/joc.1735.
- 703 Urraca, R., Gracia-Amillo, A. M., Koubli, E., Huld, T., Trentmann, J., Riihelä, A., Lind-
704 fors, A. V., Palmer, D., Gottschalg, R. and Antonanzas-Torres, F. (2017), Extensive
705 validation of CMSAF surface radiation products over Europe, *Remote Sensing of the*
706 *Environment*, *199*, 171–186, doi:10.1016/j.rse.2017.07.013.
- 707 Wild, M. and coauthors (2005), From dimming to brightening: Decadal changes in solar
708 radiation at earth’s surface, *Science*, *308*, 847–850, doi:10.1126/science.1103215.
- 709 Wild, M. (2009), Global dimming and brightening: A review, *Journal of Geophysical*
710 *Research: Atmospheres*, *114(D10)*, 2156–2202, doi:10.1029/2008JD011470.
- 711 Wild, M. (2012), Enlightening Global Dimmin and Brightening, *Bulletin of the American*
712 *Meteorological Society*, *93(1)*, 27–37, doi:10.1175/BAMS-D-11-00074.1.
- 713 Wild, M., Folini, D., Hakuba, M. Z., Schär, C., Seneviratne, S. I., Kato, S., Rutan, D.,
714 Ammann, C., Wood, E. F., and König-Langlo, G. (2015), The energy balance over land
715 and oceans: an assessment based on direct observations and CMIP5 climate models,
716 *Climate Dynamics*, *44(11-12)*, 3393–3429.
- 717 Wild, M., Folini, D., Henschel, F., Fischer, N. and Müller, B. (2015), Projections of long-
718 term changes in solar radiation based on CMIP5 climate models and their influence on

- 719 energy yields of photovoltaic systems, *Solar Energy*, 116, 12–24, doi:10.1016/j.solener.
720 2015.03.039.
- 721 Wild, M. (2016), Decadal changes in radiative fluxes at land and ocean surfaces and their
722 relevance for global warming, *Wiley Interdisciplinary Reviews: Climate Change*, 7(1),
723 91–107, doi:10.1002/wcc.372.
- 724 Wild, M., Ohmura, A., Schär, C., Müller, G., Folini, D., Schwarz, M., Hakuba, M. Z.
725 and Sanchez-Lorenzo, A. (2017), The Global Energy Balance Archive (GEBA) version
726 2017: A database for worldwide measured surface energy fluxes, *Earth System Science*
727 *Data Discussions*, doi:10.5194/essd-2017-28.
- 728 Zák, M., Mikšövský, J. and Pišoft, P. (2015), CMSAF Radiation Data: New Possibilities
729 for Climatological Applications in the Czech Republic, *Remote Sensing*, 7(11), 14445–
730 14457, doi:10.3390/rs71114445.
- 731 Zhang, X., Liang, S., Wild, M. and Jiang, B. (2015), Analysis of surface incident shortwave
732 radiation from four satellite products, *Remote Sensing of the Environment*, 165, 186–
733 202, doi:10.1016/j.rse.2015.05.015.
- 734 Zubler, E. M., Folini, D., Lohmann, U., Lthi, D., Schär, C. and Wild, M. (2011), Simula-
735 tion of dimming and brightening in Europe from 1958 to 2001 using a regional climate
736 model, *Journal of Geophysical Research*, doi:10.1029/2010JD015396.

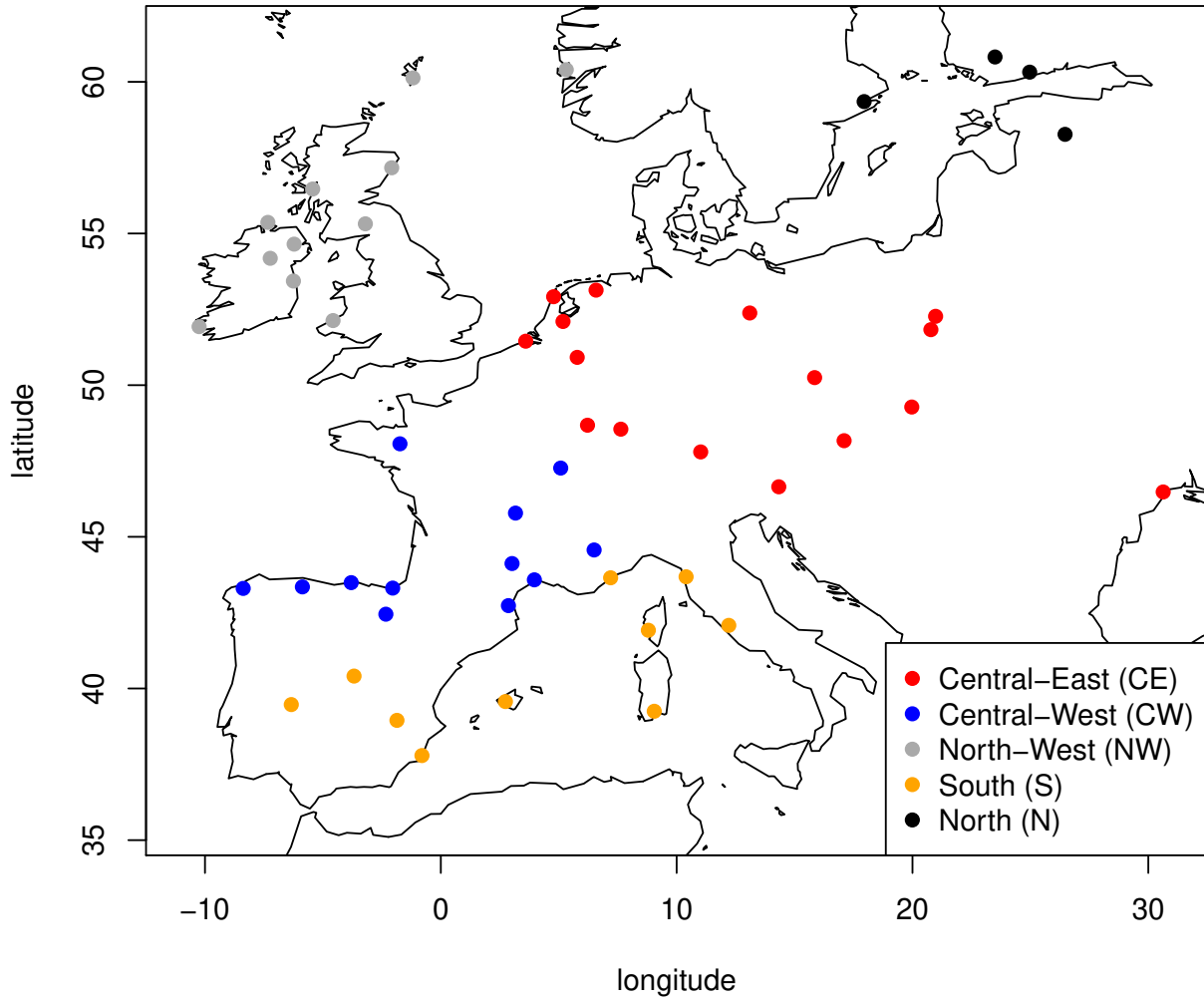


Figure 1. Stations used to evaluate satellite climate data records. The colors represent the corresponding regions as defined by a Principal Component Analysis (red - Central East, blue - Central West, grey - North-West, orange - South, black - North).

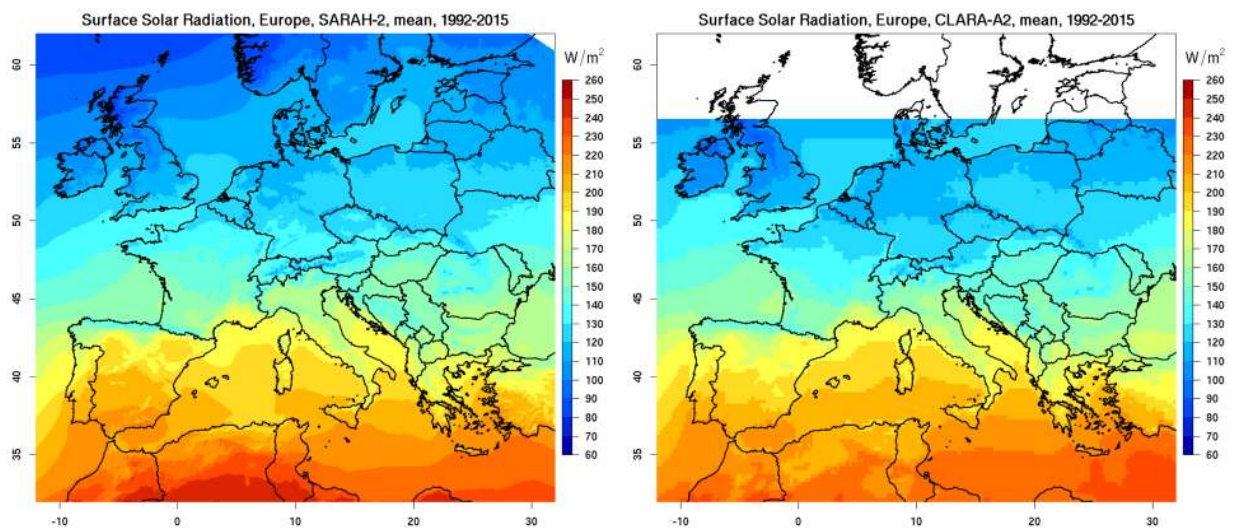


Figure 2. Mean surface solar radiation [W/m^2] (1992-2015) based on the (left) SARAH-2 and (right) CLARA-A2 climate data record.

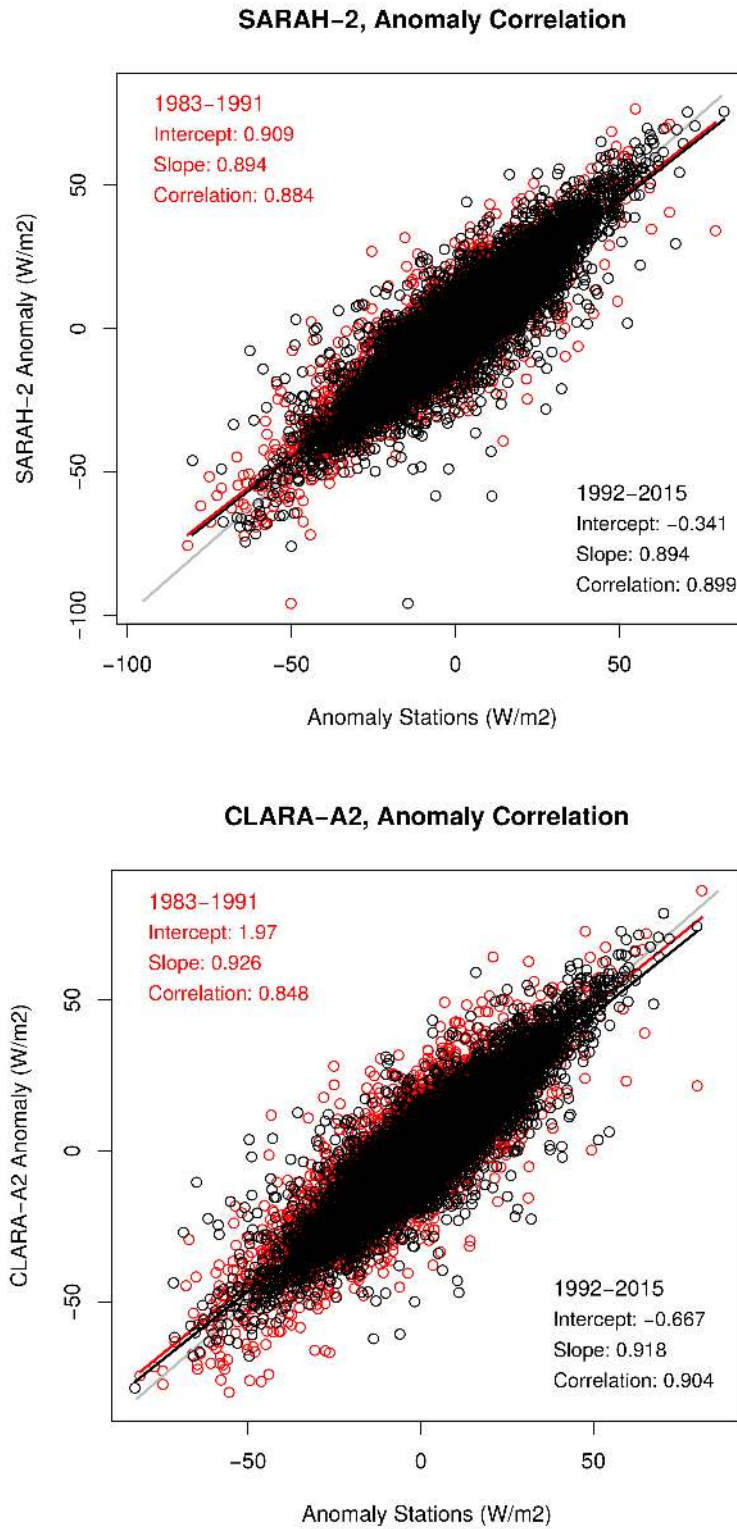


Figure 3. Scatterplot of monthly anomalies of surface solar radiation [W/m^2] of SARAH-2 (top) and CLARA-A2 (bottom) versus station data, including correlation coefficient, slope and intercept of the regression line. The red color refers to the 1983-1991 period while the black color refers to the 1992-2015 period.

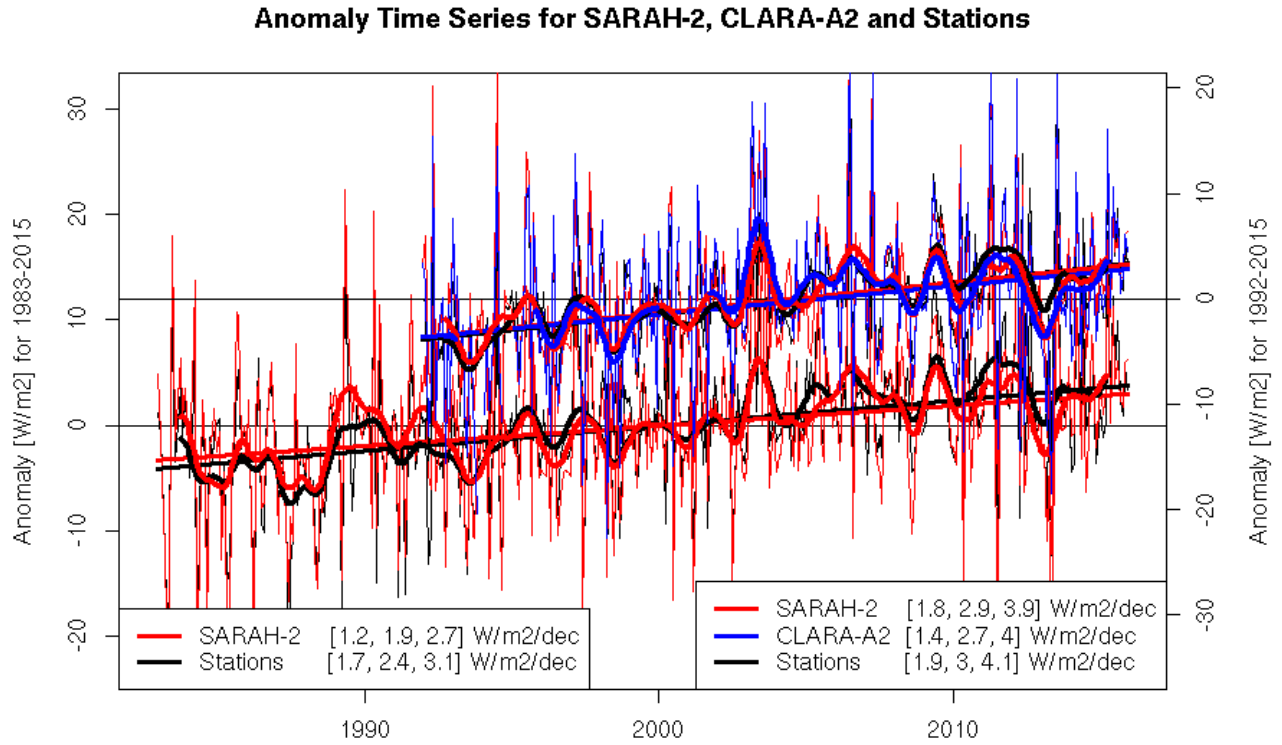


Figure 4. Mean monthly anomaly [W/m^2] time series for the time periods of 1983-2015 (lower lines, y-axes on the left) and 1992-2015 (upper lines, y-axis on the right). Additionally shown are the linear trends (solid straight lines) and the smoothed time series (using 12-month Gauss-filter) for (black) Stations, (red) SARAH-2 and (blue) CLARA-A2 (only for the time period 1992-2015). The values in the brackets show: lower 95%-percentile, mean trend, upper 95%-percentile. **Note** that the y-axis are shifted by $12 W/m^2$ from each other.

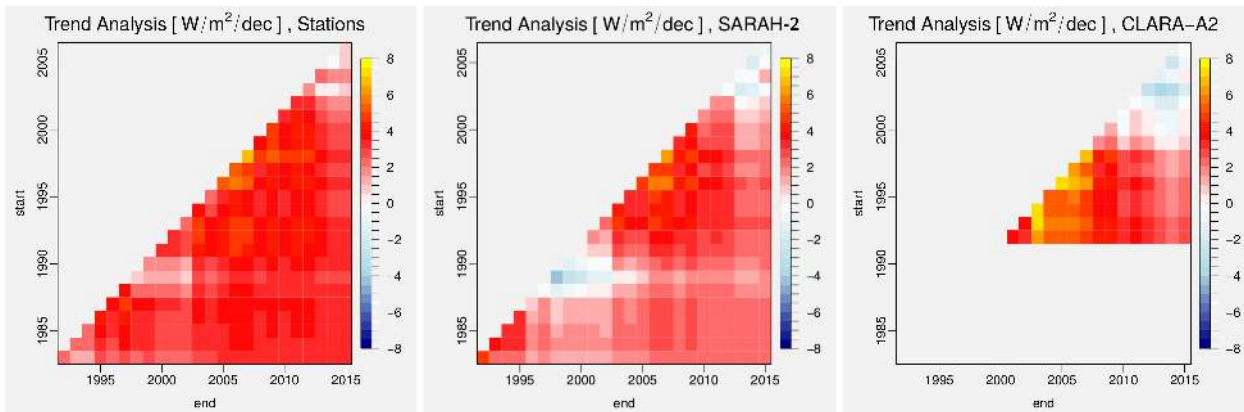


Figure 5. Trendraster-Plots of mean SSR trends derived from Stations (left), SARAH-2 (middle) and CLARA-A2 (right). The y-axis denotes the start-years and the x-axis shows the end-years of the individual trends, respectively. Trendrasters show linear trends [$W/m^2/decade$] during time periods of at least 10 years (at the diagonal); the trend over the maximum time period analysed (33 years for station data and SARAH-2; 24 years for CLARA-A2) is shown by the pixel at the lower right end.

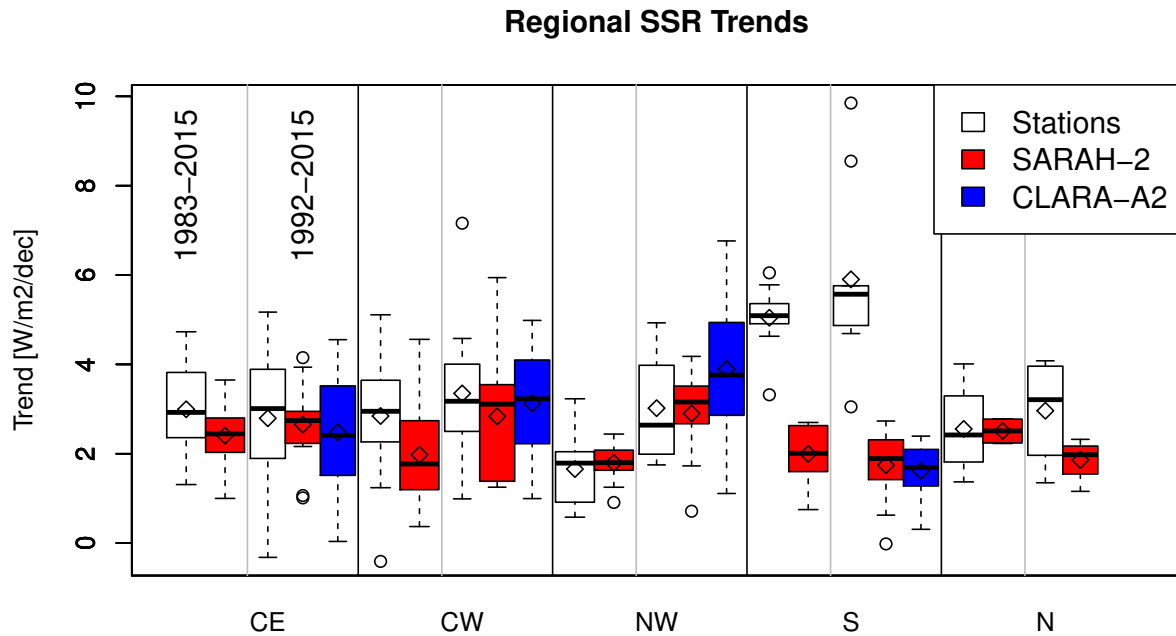


Figure 6. Boxplot of the regional trends [$W/m^2/decade$] of surface solar radiation at the station locations (white) based on Stations, (red) SARAH-2, and (blue) CLARA-A2 data, including mean trends (diamonds). Outliers are shown as dots. Regions: CE=Central East, CW=Central West, NW=North West, S=South, N=North. For each region the plot area is divided into trends for the full time period 1983-2015 (for Stations and SARAH-2) and trends for the time period 1992-2015 (for Stations, SARAH-2 and CLARA-A2).

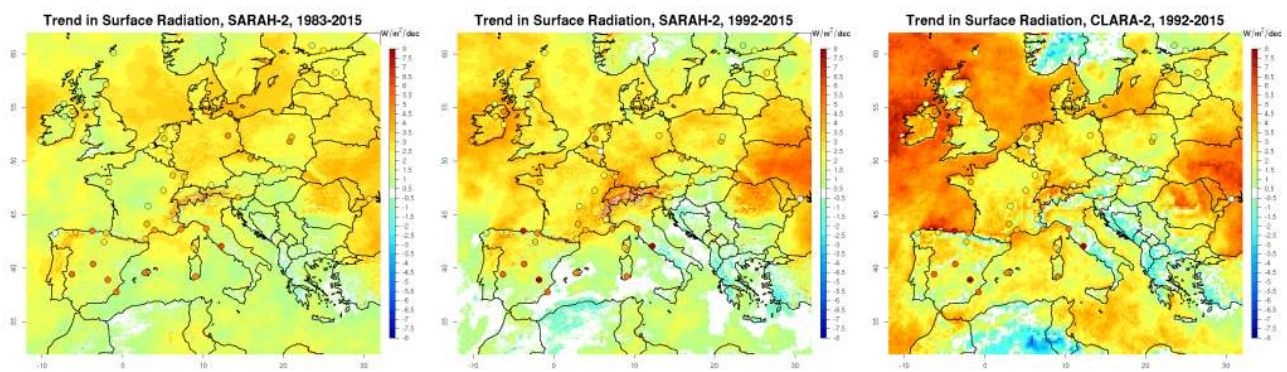


Figure 7. Spatial distribution of the linear trends [$W/m^2/decade$] of surface solar radiation during 1983-2015 for (left) SARAH-2 and during 1992-2015 for (center) SARAH-2 and (right) CLARA-2. The respective trends for the 53 stations are shown as coloured dots.

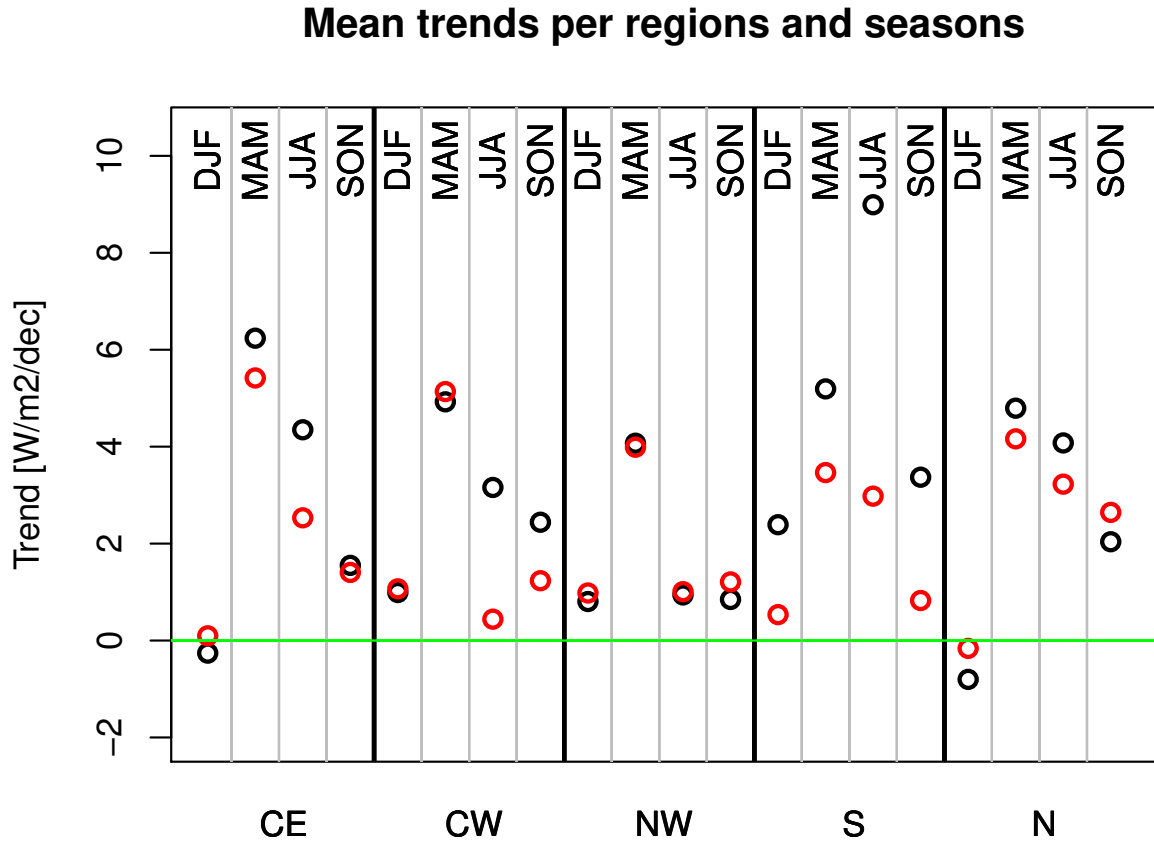


Figure 8. Trends [$W/m^2/decade$] of surface solar radiation of (black) Stations and (red) SARAH-2 data, shown separately for region and season during the full time period of 1983-2015. Regions: CE=Central East, CW=Central West, NW=North West, S=South, N=North.

Mean trends per regions and seasons

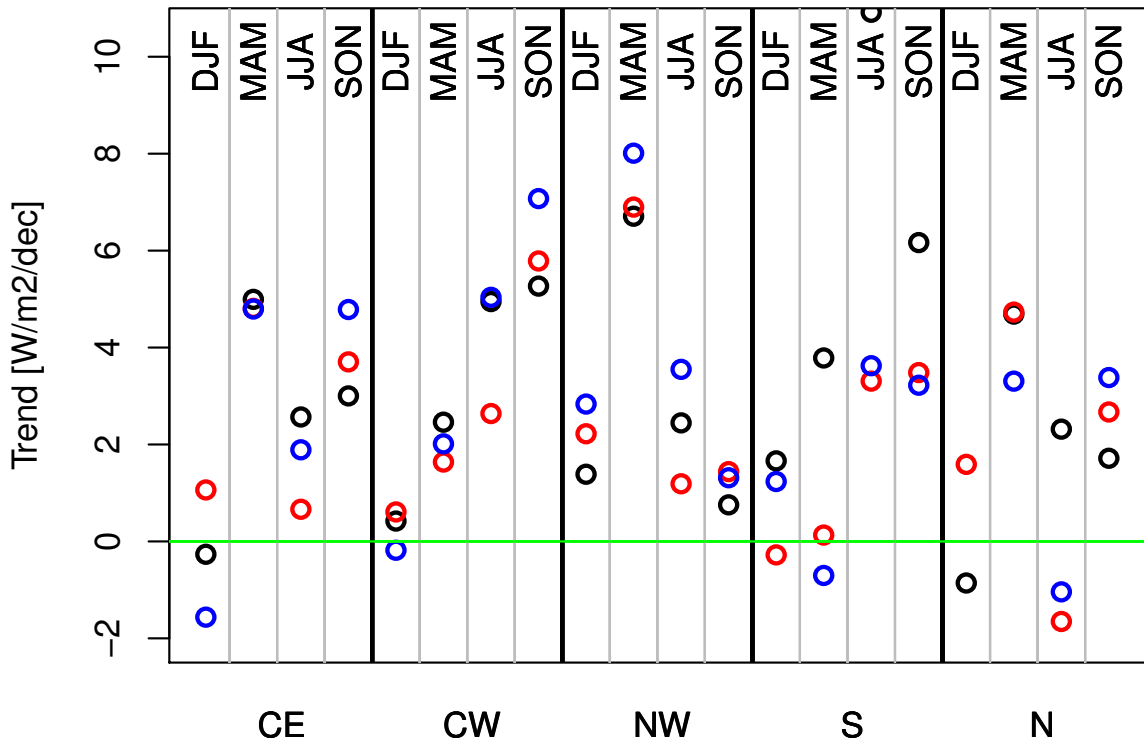


Figure 9. Trends [$W/m^2/decade$] of surface solar radiation of (black) Stations, (red) SARA-H2 and (blue) CLARA-A2 data, shown separately for region and season during the time period of 1992-2015. Regions: CE=Central East, CW=Central West, NW=North West, S=South, N=North.

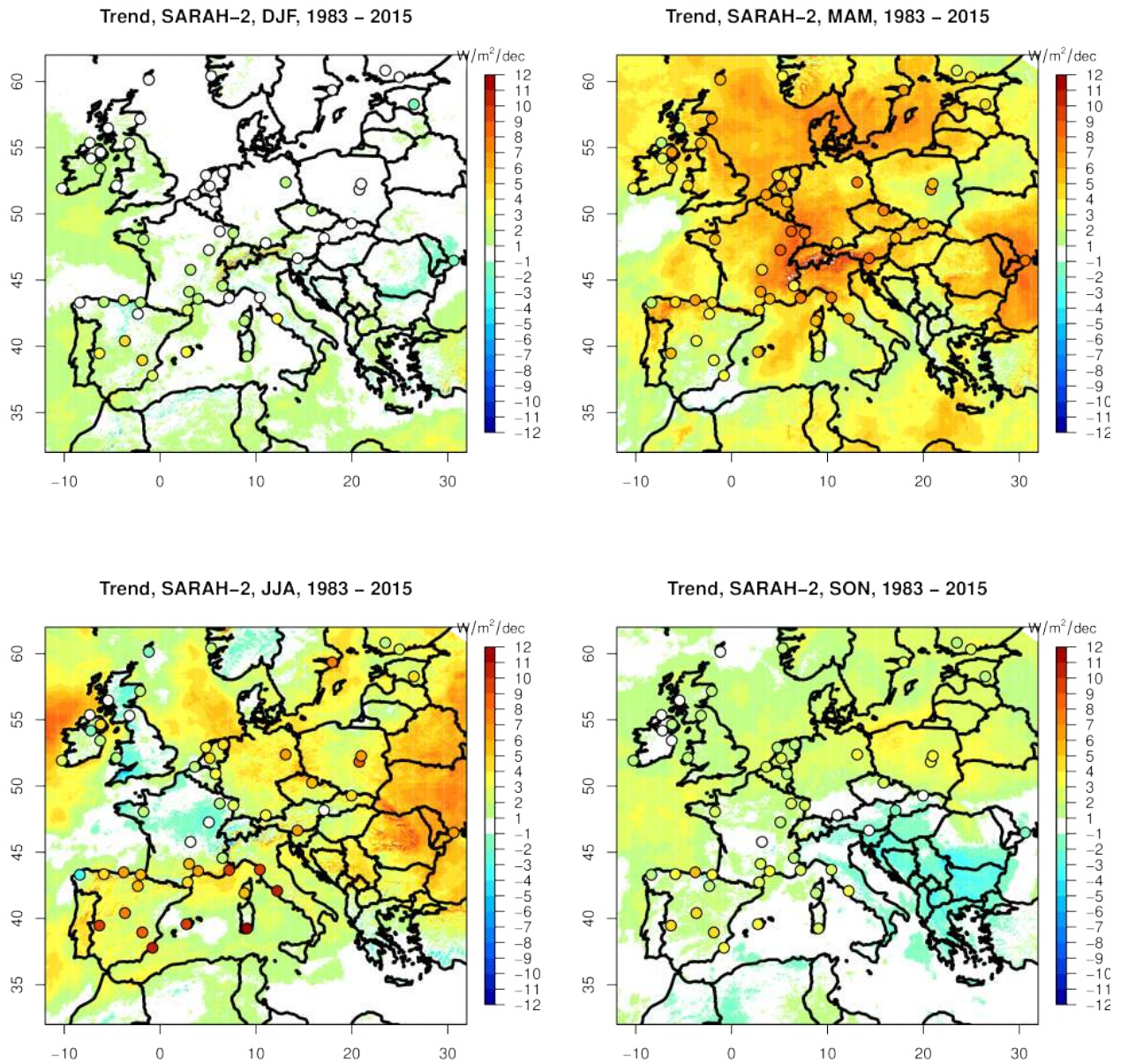


Figure 10. Spatial distribution of the linear trends [$W/m^2/decade$] of surface solar radiation during 1983-2015 for the four seasons (DJF, MAM, JJA, SON) based on the SARAH-2 climate data record. The trends for the respective season and time period given by the 53 stations are shown as coloured dots.

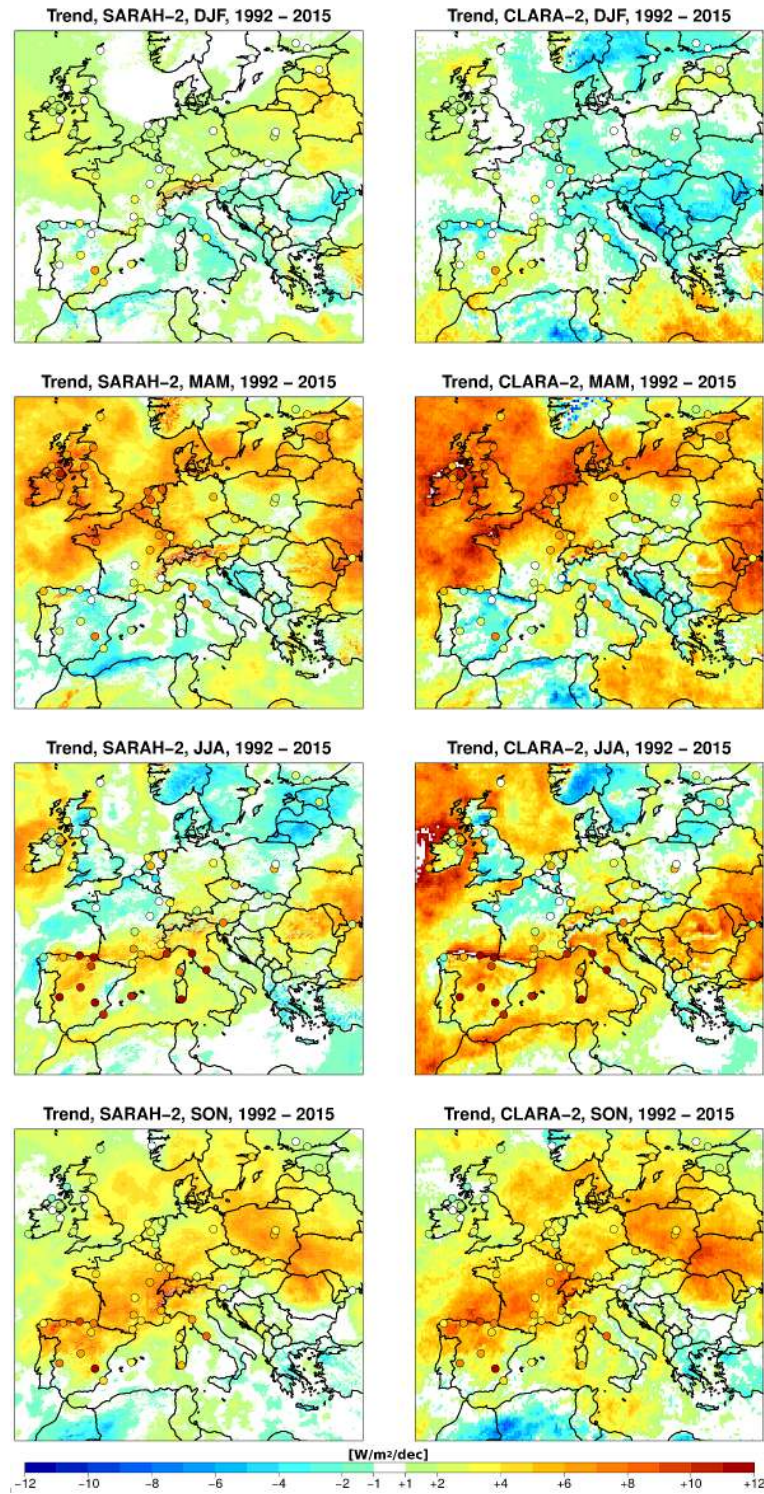


Figure 11. Spatial distribution of the linear trends [$W/m^2/decade$] of surface solar radiation during 1992-2015 for the four seasons (DJF, MAM, JJA, SON) (top to bottom) based on the (left) SARAH-2 and (right) CLARA-A2 climate data records. The trends for the respective season and time period given by the stations are shown as coloured dots.

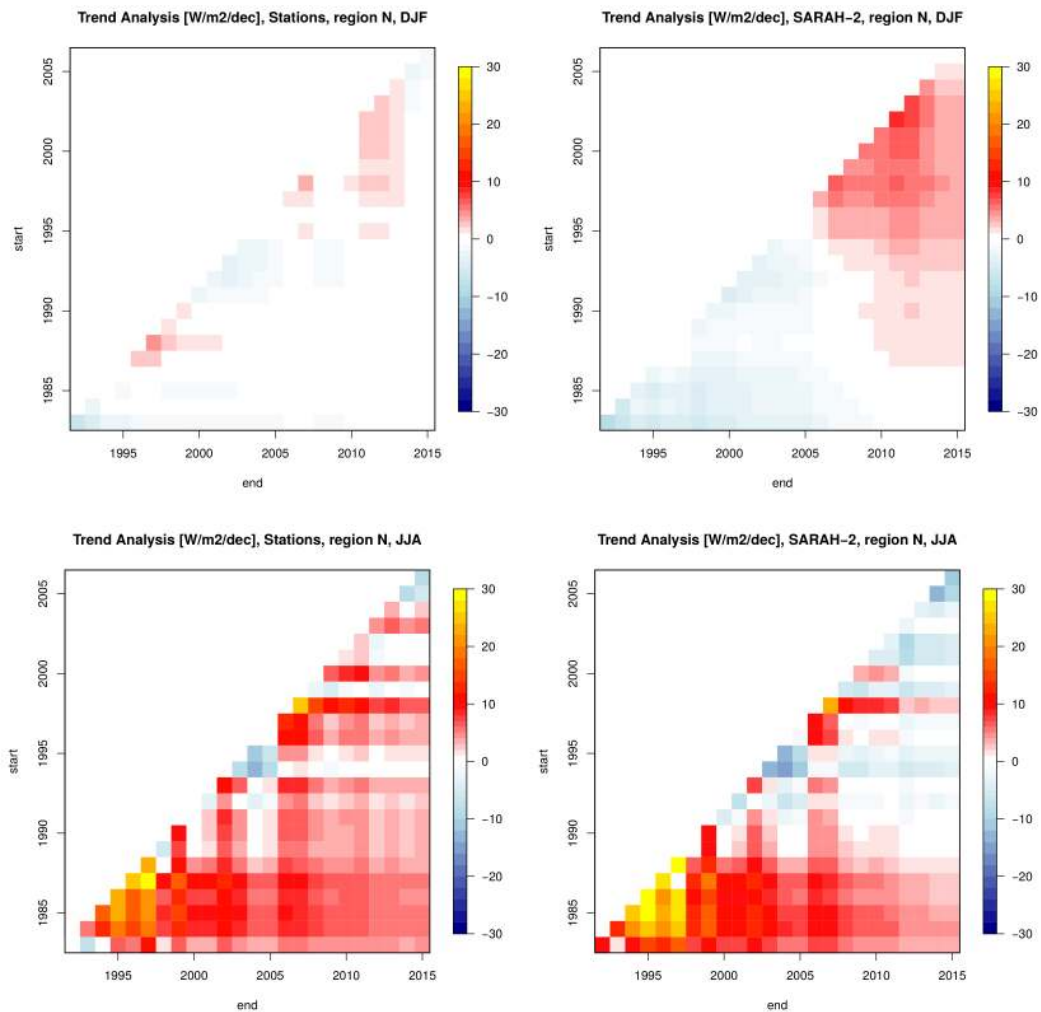


Figure 12. Trendraster-Plots of mean SSR trends derived from (left) Stations and (right) SARA-2, for the (top) winter and (bottom) summer season for the region North. The y-axis denotes the start-years and the x-axis shows the end-years of the individual trends, respectively. Trendrasters show linear trends [$W/m^2/decade$] during time periods of at least 10 years (at the diagonal); the trend over the maximum time period analysed is shown by the pixel at the lower right end.

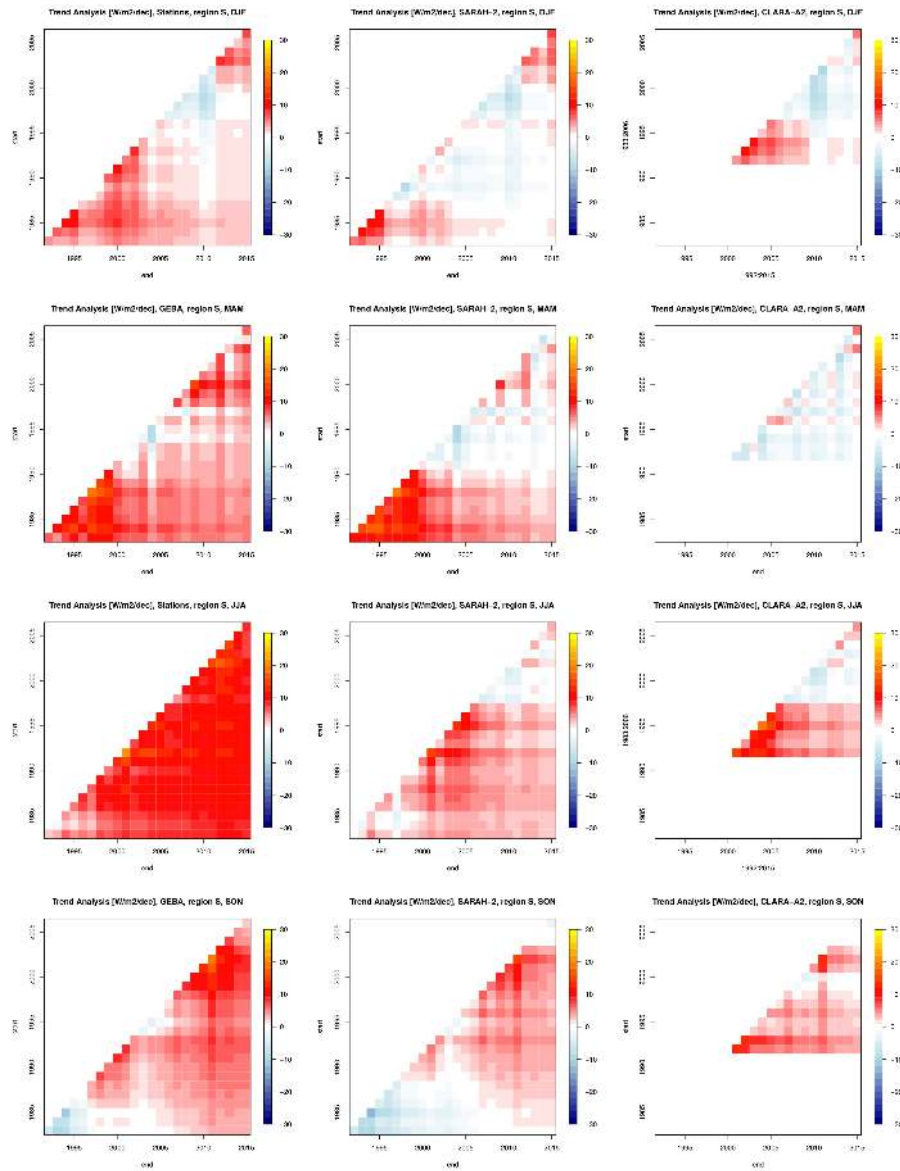


Figure 13. Trendraster-Plots of mean SSR trends derived from (left) Stations, (center) SARAH-2 and (right) CLARA-A2 for the seasons (from top to bottom: DJF, MAM, JJA, SON) for the region South. Trendrasters show linear trends [$W/m^2/decade$] during time periods of at least 10 years (at the diagonal); the trend over the maximum time period analysed (33 years for station data and SARAH-2; 24 years for CLARA-A2) is shown by the pixel at the lower right end.

Table 1. List of the 53 stations used in this study.

Station	Lon [°W]	Lat [°N]	Country	Region
Aberdeen	-2.083	57.167	Great Britain	NW
Aberporth	-4.570	52.130	Great Britain	NW
Ajaccio	8.800	41.920	France	S
Albacete	-1.860	38.950	Spain	S
Aldergrove	-6.220	54.650	Great Britain	NW
Belsk	20.780	51.830	Poland	CE
Bergen	5.320	60.400	Norway	NW
Bratislava	17.100	48.170	Slovak Republic	CE
Caceres	-6.340	39.470	Spain	S
Cagliari	9.050	39.250	Italy	S
Clermont-Ferrand	3.167	45.783	France	CW
Clones	-7.233	54.183	Ireland	NW
Coruna	-8.380	43.300	Spain	CW
De Bilt	5.180	52.100	Netherlands	CE
De Kooy	4.783	52.917	Netherlands	CE
Dijon	5.083	47.267	France	CW
Dublin	-6.250	53.433	Ireland	NW
Dunstaffnage	-5.433	56.467	Great Britain	NW
Eelde	6.583	53.133	Netherlands	CE
Embrun	6.500	44.567	France	CW
Eskdalemuir	-3.200	55.320	Great Britain	NW
Helsinki	24.970	60.320	Finland	N
Hohenpeissenberg	11.020	47.800	Germany	CE
Hradec-Kralove	15.850	50.250	Czech Republic	CE
Jokioinen	23.500	60.820	Finland	N
Klagenfurt	14.330	46.650	Austria	CE
Lerwick	-1.180	60.130	Great Britain	NW
Logrono	-2.330	42.450	Spain	CW
Maastricht	5.783	50.917	Netherlands	CE
Madrid	-3.680	40.410	Spain	S
Malin-Head	-7.333	55.367	Ireland	NW
Millau	3.020	44.120	France	CW
Montpellier	3.967	43.583	France	CW
Murcia	-0.800	37.790	Spain	S
Nancy-Essey	6.220	48.680	France	CE
Nice	7.200	43.650	France	S
Odessa	30.630	46.480	Ukraine	CE
Oviedo	-5.870	43.350	Spain	CW
Palma de Mallorca	2.740	39.570	Spain	S
Perpignan	2.867	42.733	France	CW
Pisa	10.400	43.683	Italy	S
Potsdam	13.100	52.380	Germany	CE
Rennes	-1.733	48.067	France	CW
San Sebastian	-2.040	43.310	Spain	CW
Santander	-3.800	43.490	Spain	CW
Stockholm	17.950	59.350	Sweden	N
Strasbourg	7.633	48.550	France	CE
Toravere	26.470	58.270	Estonia	N
Valentia	-10.250	51.930	Ireland	NW
Vigna di Valle	12.211	42.081	Italy	S
Vlissingen	3.600	51.450	Netherlands	CE
Warszawa	20.980	52.270	Poland	CE
Zakopane	19.970	49.280	Poland	CE

Table 2. Results of the validation of monthly SARA-H-2 and CLARA-A2 surface radiation data with reference to station data in Europe. MAD=Mean Absolute Deviation [W/m^2], cor=Pearson's correlation coefficient of the anomaly series

	1983-1991		1992-2015		1983-2015	
	MAD	cor	MAD	cor	MAD	cor
CLARA-A2	9.7	0.85	6.5	0.91	7.3	0.88
SARA-H-2	8.3	0.89	6.4	0.90	6.9	0.89

Table 3. Absolute [$W/m^2/decade$] and relative [$\%/decade$] trends of SARA-H-2, CLARA-A2 and the station data during the time periods of 1983-2015 and 1992-2015 for the five regions analysed.

time period	data	CE	CW	NW	S	N
1983-2015	Stations	3.0 (2.4%)	2.9 (1.9%)	1.7 (1.6%)	5.0 (2.7%)	2.6 (2.4%)
	SARA-H-2	2.4 (1.9%)	2.0 (1.3%)	1.8 (1.8%)	2.0 (1.0%)	2.5 (2.4%)
1992-2015	Stations	2.6 (2.0%)	3.3 (2.2%)	2.8 (2.7%)	5.7 (3.0%)	2.0 (1.8%)
	SARA-H-2	2.7 (2.0%)	2.8 (1.8%)	2.9 (2.9%)	1.8 (0.9%)	1.9 (1.7%)
	CLARA-A2	2.4 (1.8%)	3.1 (2.0%)	3.7 (3.4%)	1.9 (1.0%)	/